


Review

A Review of Green Scale Inhibitors: Process, Types, Mechanism and Properties

Mohammad A. Jafar Mazumder 

Chemistry Department, King Fahd University of Petroleum and Minerals, Dhahran 31261, Saudi Arabia; jafar@kfupm.edu.sa; Tel.: +966-13-8607836

Received: 8 August 2020; Accepted: 24 September 2020; Published: 28 September 2020



Abstract: In the present time, more often, it has been seen that scaling has grown as widely and caused problems in the oilfield industry. Scaling is the deposition of various salts of inorganic/organic materials due to the supersaturation of salt-water mixtures. Many works have been proposed by researchers using different methods to solve the problem, of which scale inhibition is one of them. The scale inhibitors, particularly for antiscaling, have derived from natural and synthetic polymers. Among different polymers, inorganic and organic compounds (polyphosphates, carboxylic acid, ethylenediaminetetraacetic acid (EDTA), etc.) can effectively manage the oilfield scales of which many are toxic and expansive. Scale inhibitors of alkaline earth metal carbonate and sulfates and transition metal sulfide are commonly used in oilfield applications. Scale inhibition of metallic surfaces is an essential activity in technical, environmental, economic, and safety purposes. Scale inhibitors containing phosphorus appear to have significant achievements in the inhibition process despite its toxicity. However, phosphorus-based inhibitors can serve as supplements prompting eutrophication difficulties. Besides these increasing environmental concerns, green scale inhibitors are renewable, biodegradable, and ecologically acceptable that has been used to prevent, control, and retard the formation of scale. Considering the facts, this review article summarized the concept of scale, various green scale inhibitors, types, mechanisms, comparative performance, significance, and future aspects of green scale inhibitors, which will shed light and be helpful for the professionals working in the oil and gas industries.

Keywords: green scale; scale inhibitors; types; inhibition process; inhibition mechanism; antiscalants

1. Introduction

Nowadays, corrosion and scaling are fundamental problems in the area of industrial wastewater treatment. This water mainly contains salts of inorganic materials and corrosion metal (Fe), which leads to scaling on the surface of the metal, equipment damage and a waste of energy. Various scale inhibitors have usually been added to the circulating cold water, which is considered the most effective measure to increase the utilization rate, reduce the scale and corrosion of the equipment, and save water and energy. Scale inhibitors can circularize the insoluble inorganic salts, prevent scale deposition on the metal surface, which slows down the corrosion rate, and maintains proper heat transfer effect of the equipment. These inhibitors are considered a particular class of chemicals, which are also used to slow or stop scale development in water frameworks [1–5]. Researchers also studied different types of scales and methods to prevent them from using scale inhibitors. In most cases, it has been seen that the scale dissolver is required even subsequent to using scale inhibitors to remove scale or corrosion, which is treated as an essential control technique. In scale prevention, there are numerous postulates where the inhibitor's function is not very useful. The expectation of the development of scale doesn't precisely guarantee that it relies on the solvency of saltwater when the arrangement of the inhibitor is nonideal and inferable due to the reservoir heterogeneity [5–7]. Scale affidavit in down-hole surfaces

started because of the performance of the nearby saline solution in nature and the low solvency of a portion of the generated inorganic salt. Scale deposition is led by three types of mechanisms in on/offshore areas: (a) mixing of two incompatible brines, (b) changes in conditions like pressure and temperature, and (c) evaporation of brine [8].

Water is highly compatible with brine due to the chemical interaction between the two. When it is mixed, precipitates are formed and deposit the scale. Seawater (consisting of low/high concentration of alkaline metal/sulfate ions) and formation-water (consisting of high/low level of alkaline metal/sulfate ions) are typical examples of incompatible brines. Scale only forms when water is produced. Water has prime importance in inhibiting scale in oilfield applications. These common waters are high in ions because of the disintegration of various mineral constituents. The formation comprises of generous amounts of different alkaline metal cations by the dissolution of total solids approaching 4000 g L^{-1} . Scale precipitation of the sulfates contains Ca, and Ba is due to the mixing of these types of mineral-rich water. Besides, the other incompatible brine results in the sulfide types of brine appear by the reaction of H_2S with another metal (Fe, Zn, Pb, etc.) [9–13].

The deposition of scale relies upon several factors such as reaction equilibria, pressure, temperature, pH, evaporation, exposure time, and salt concentration. Scale deposition could be due to single minerals or composed of the combination of various elements. Some organic/inorganic compounds such as unsaturated aliphatic/aromatic hydrocarbons, aromatic sulfur-containing compounds, paraffin, resins, naphthenic acids, and their salts may also affect scale formation in down-hole conditions. A few compounds of alkaline and transition metals (Mg, Ca, Fe) in the form of oxides/hydroxides/carbonates/sulfates are also encountered in scale formation in the oil and gas industry [14–17]. The various typical scale compositions in carbonates and sandstone reservoirs were presented in earlier published literature [9]. A number of researchers' investigations showed how scale dissolver (remover) can be applied to dissolve the scale. In contrast, scale inhibitors can be used to prevent scale formation. A group of researchers [14] studied the mechanism and properties of scale development in wastewater treatment and water desalination process by reverse osmosis (RO). Li et al. have made other investigations for scale formation and prevention of scale using inhibitors [15]. Besides these, several researchers have also focused on scale formation and prevention using various methods, such as gas wells and oilfield scale management technology. They discussed thermodynamic and kinetic prediction and physical causes of scale formation during production operations of mineral scale formation. This study also reveals that water has been taken as a significant source for all types of scales. When water is produced along with oil and gas, various scales are relied upon to shape the production tube or the reservoir. The deposition of scale in the inner side of the wellbore tubing diminishes the width of the production pipe, obstructing and hindering the flow. It might cause a serious pressure drop and, accordingly, a lessening of the efficiency of the well as discussed by Olajire et al. [5]. They reported that the production capacity reached zero within a few hours, and the treatment of this system causes an immense cost. This study suggested that the blockage of various pipelines, damage in the reservoir, and increasing corrosion rate may cause the precipitation of scale and pose a threat to safe production operations [5,18–22].

Inorganic scale inhibitors play an oxidizing agent on the metal surface and form a passive membrane on the active sites of the surface. However, some inorganic inhibitors, namely nitrate- and chromate-based inhibitors, are found to be cost-effective but are toxic and unsafe. The most environmentally acceptable materials gradually terminate them [23]. Enormous efforts have been made by the scientific community to find environmentally friendly and less wearing alternatives that lower adverse effects on the ecosystem. A few nontoxic and cost-effective alternatives, such as molybdates, silicates, phosphate/polyphosphates, and zinc salts, are found to be the best replacement for nitrate and chromate-based inhibitors.

The inhibition activity of organic inhibitors can also be substantially upgraded using transition metal cations. Several researchers [21–24] have extensively studied the possible synergistic effects between the organic scale inhibitors and the particular transition metal cations. Among different

transition metal cations, the Zn^{2+} ion with organic scale inhibitors has been extensively studied due to their multifunctional properties. In the class of organic scale inhibitors, natural and synthetic polymeric inhibitors are usually used as dispersants in the inhibition process. The dominant type of synthetic polymers, such as acrylamide, acrylic acid, methacrylic acid, and malic acid, having a molecular weight of 50 kDa, are well known as dispersants. The effectiveness of these inhibitors depends on the chain length of the polymers. The efficiency is found to be low for higher chain length; in most cases, the polymers having repeating units of approximately 10–15 are considered a suitable scale inhibitor [24–28]. In general, the low-molecular-weight acrylate and organophosphorus-based polymers are mostly used in scale inhibition. Poly amino polyether methylene phosphonate (PAPEMP) is a very effective inhibitor in preventing CaCO_3 precipitation [29,30]. The extraordinary affinity of PAPEMP towards CaCO_3 surfaces and its excellent tolerance of calcium materials make this polymer excellent in inhibiting the growth of CaCO_3 crystal. Amjad et al. have extensively studied phosphonate-based polymer performance in cold water [29]. They have studied the effectiveness of phosphate and phosphonate polymers in stabilized and all-organic cooling water treatment facilities. This study reported that these polymers are capable of performing a dual function. Firstly, they control the thickness of the calcium phosphate and phosphonate membrane on the metal surface. Secondly, they prevent the precipitation of the calcium phosphate and phosphonate salts in the recirculating water [29–33]. Another study conducted by the same research group demonstrated the performance of sulphonic-acid-containing terpolymer for controlling the growth of calcium phosphonates and carbonate scale. It showed that these polymers improved the control of calcium phosphonate and carbonate in highly stressed cooling water systems [28]. Wang et al. also conducted a similar study in which they have reported the inhibition of CaCO_3 by a phosphonate-terminated poly(maleic-co-sulfonate) polymeric inhibitor. This study showed that this inhibitor is capable of controlling CaCO_3 scale [31].

Several studies have been conducted using nonaqueous scale inhibitors, namely water-free materials in organic solvent blends, oil-soluble inhibitors, microemulsion or nanoemulsions, and inverted emulsion-encapsulated products. Microemulsions are a typical surfactant mixed with thermodynamically stable microdispersed materials formed by mixing of water and oil with no or little energy inputs based on their thermodynamic stability. Mostly, microemulsions are of two types: o/w (i.e., micelle) and w/o (i.e., reverse micelle) and can spontaneously form in the presence of surfactants. The necessary condition for microemulsion is to develop a low interfacial tension between the oil and water so that dispersion forces can overcompensate the remaining interface free energy. Several researchers have studied phosphonate nanomaterial in microemulsions for scale inhibition and discussed the retention mechanisms of these nonaqueous inhibitor products [16,34–39].

The process of water reclamation, i.e., desalination process, membrane filtration, and recirculating cooling water systems, is mostly used at industrial scale in which scales widely exist. These processes run in the long term, cause formation and deposition of scales that remain an obstacle, and decrease the heat transfer efficiencies, speed up membrane fouling, and even cause catastrophic accidents. Most studied metal ions of Ca, and Fe bear the formation of scales that originate from hard water, biological activities, corrosion, and chemicals used for the purification of ferric water [40,41]. Among various generations of scales from these studied metals ions, the ferric oxide/hydroxides and $\text{Ca}_3(\text{PO}_4)_2$ appeared to be the most effective inhibitors due to their low solubility product values (K_{sp} ; $\text{Fe}(\text{OH})_3 = 1.1 \times 10^{-36}$; $\text{Ca}_3(\text{PO}_4)_2 = 2.1 \times 10^{-33}$). On the other hand, the K_{sp} values of other salts (sulfates, carbonates, etc.) of these metal ions are calculated to be $\text{CaSO}_4 = 4.9 \times 10^{-5}$; $\text{CaCO}_3 = 3.4 \times 10^{-9}$; $\text{FeCO}_3 = 3.1 \times 10^{-11}$; $\text{Fe}_3(\text{PO}_4)_2 = 9.91 \times 10^{-14}$. Despite the low K_{sp} value of phosphates and oxides inhibitors, there are some challenges that still exist in the inhibition of scale and corrosion against $\text{Fe}(\text{OH})_3$ and $\text{Ca}_3(\text{PO}_4)_2$ [42]. Scale inhibitors containing phosphorus appear with significant achievements in the inhibition process despite its toxicity. An alternative of phosphorus-free (P-free) inhibitors is receiving huge interest in development depending on the regulatory limitation concerning water metamorphosis. Polymer type P-free inhibitors, e.g., polyacrylic acid, are applied in the inhibition process [42]. To evaluate the performance of an inhibitor, one should consider the following factors: (a) the inhibitors should form

strong binding interactions with target metal ions and compete with phosphate and hydroxide anions, and (b) ensure the high stability of inhibitor-metal complex formation. More often, when negatively charged carboxyl groups in a polyacrylic acid bind with metal cations, charge neutralization would occur, which destabilizes inhibitor-metal-ion complexes and promotes the formation and sedimentation of aggregates. It is worthwhile to mention that scale inhibitors based on phosphorus (phosphonates, organic phosphorus-containing polymers, etc.) are mostly used in China. However, these polymeric compounds mixed with wastewater result in the ecological imbalance in water, equipment damage, and environmental pollution [43–46].

Concerning all these constraints, the present review work has focused on the environmentally friendly scale inhibitors that treat water efficiently, which has become a challenging task in recent research. At the beginning of the 20th century, the US Betz laboratory and Proctor and Gamble developed a biodegradable, nonphosphorus and nitrogen-free “green” water agent, polyepoxysuccinate, with dual properties of dispersion and scale inhibition with broader application prospects. Following their development, many researchers conducted extensive studies on the successful synthesis of P-free-type inhibitors and their multiscale inhibition. Given these prospects, this review article summarized the concept of scale, scale inhibitors, types, mechanism, significance and properties of green scale inhibitors that will be helpful for the professionals working in the oil and gas industries.

2. Scaling Process

Some fundamental points require consideration in the development of the scaling process on the surface. The scaling process involves the following stages:

2.1. Initiation

In the initiation process, the surface is conditioned for a specified period, and the initial period is usually affected by a few factors concerning the surface, such as roughness, finishing and coating of the surface, material and its temperature, and the flow rate and scaling concentration of the solution. The formation of nuclei for the deposition of crystals is found during the induction period. This period has no fixed time interval; it may take a few seconds or minutes or a couple of hours or even a week. The induction period is inversely proportional to the supersaturation degree or the surface temperature. Due to the acceleration of induction reactions, the delay period decreases with increasing temperature. An increase in temperature tends to give more energy to get better activation energy of the precipitation reaction and accelerate the scale segments' transport from the bulk solution for the surface. As the surface irregularity increases, it will diminish the delay period [47–50].

2.2. Transport

Transportation of the scaling substances occurs from the bulk liquid to the surface over the periphery layer. It depends upon the physical properties of the system, bulk concentration, and the fluid surface interface. Transport is affected by sedimentation, diffusion, and thermophoresis physical phenomena. A relationship can be established on the surface to the local deposition flux m_d as [50] described in Equation (1)

$$m_d = h_D(C_b - C_w) \quad (1)$$

where, C_b and C_w are the reactant concentrations in the bulk solution and the solution adjacent to the surface. h_D is the mass transfer coefficient that is obtained from the Sherwood number (S_h) [50], which is related to the flow and the geometric parameters by Equation (2) as

$$S_h = h_D L / D \quad (2)$$

where L and D are a length in meters and mass diffusivity in m^2s^{-1} .

2.3. Deposition

This part comprises a scale deposit that is compared between itself and to the surface. Salt ions approaching the surface of scales interact with it due to electromagnetic forces. It corresponds to the nucleation formation to the surface and gently develops with time to form scale layers. Thus, the action of the electromagnetic forces on the particles as they approach the surface is significant in influencing the attachment. The material characteristics, including density, size, and surface conditions, change the attachment [50].

2.4. Removal

There is a contest between deposition and removal of the scale materials. The scalants usually deposit on the surface up to a particular level on a regular increment. At the interfaces, the shear forces between the fluid and scales stored are accountable for removal. The viscosity of the liquid, velocity gradients at the surface, and roughness of the surface are directing the shear forces. Removal performance occurs from the surface via a mechanism of dissolution, erosion, and spalling [50].

2.5. Aging

The process of aging starts with the beginning of the deposition of scale, and alteration of the crystal may occur to decrease or improve the strength of deposition with time during the aging process. The change in chemical or crystal structure can influence the mechanical properties of the deposit. Commencement of the chemical composition of the deposit may change its mechanical strength [50].

3. Types of Scales

The formation of scale depends on the depth or height of the well. It varies from one to another well or height of a similar well. The oilfield scales are not limited but mainly classified as sulfides and oxides of iron, sulfates, and carbonates of calcium and magnesium, etc. [51]. Kamal et al. reported these types of oilfield scales in their study and they are listed in Table 1 [9]. The tendency of scaling of these scales can be dependent on or independent of the brine pH. The sulfide and carbonate scales are dependent while barites and sulfates are not dependent on the brine pH. Commonly, a large portion of the scales is dissolvable in either water or corrosive, while a few scales do not show their solvency in water or acids. For example, the NaCl scale shows solubility in the water, while CaCO_3 , FeS, FeO are soluble in acid [52,53].

Table 1. Different Types of Scales.

Scale Type	Scale
Sulfides	
Pyrrhotite	Fe_7S_8
Troilite	FeS
Mackinawite	Fe_9S_8
Pyrite	FeS_2
Marcasite	FeS_2
Greigite	Fe_3S_4
Sphalerite	ZnS
Galena	PbS
Sulfates	
Gypsum	$\text{CaSO}_4 \cdot 2\text{H}_2\text{O}$
Anhydrite	CaSO_4
Barite	BaSO_4
Hemihydrate	$\text{CaSO}_4 \cdot 0.5\text{H}_2\text{O}$
Celestite	SrSO_4

Table 1. Cont.

Scale Type	Scale
Carbonates	
Calcite	CaCO_3
Vaterite	CaCO_3
Aragonite	CaCO_3
Siderite	FeCO_3
Dolomite	$\text{CaMg}(\text{CO}_3)_2$
Iron scales	
Ferrous Hydroxide	$\text{Fe}(\text{OH})_2$
Ferrous Hydroxide	$\text{Fe}(\text{OH})_3$
Hematite	Fe_2O_3
Magnetite	Fe_3O_4
Akaganeite	$\alpha\text{-FeOOH}$
Goethite	$\beta\text{-FeOOH}$
Lepidocrocite	$\gamma\text{-FeOOH}$
Hibbingite	$\text{Fe}_2(\text{OH})_3\text{Cl}$

3.1. Sulfide Scales

3.1.1. Iron Sulfide

This type of scale is generally formed in sour oil and gas wells. Substantial variations are found as it can change from fluidic to powder. The behaviors of this scale are mainly as functions of scale age, temperature, pressure, and brine pH. The reaction of iron with H_2S produces iron sulfide precipitates as iron is in ionic form and H_2S in gaseous form [54]. Many researchers have reported the sources to deliver the H_2S and Fe in the wells, such as reduction of sulfate ion, acid treatment of sour wells, degradation of drilling mud additives, thermal degradation of organic sulfur-containing compounds, and sulfate-reducing bacteria. It may be generated as free gas in sour wells. The thermal degradation of sulfate-containing minerals can also afford hydrogen sulfide.

Similarly, iron can also be obtained from various sources such as leaching of iron from minerals, propping agents, tubular arrangement, saline solution dirt, and a few other liquids lost during boring and culmination processes in which leaching is the primary source. Ores of iron are also the familiar sources from which iron can be obtained in the formation of scales where hematite is a sedimentary ore, consisting of hematite ore up to 2% by weight and typically found in sandstone reservoirs. Several researchers have reported an additional source of iron in the well by introducing proppant during hydraulic fracturing processes [55,56].

Based on the iron-to-sulfur ratio, iron sulfide scales are found in different forms depending on temperature, pressure, formation mineralogy, exposure time, brine, and pH. These scales are reported as either monosulfide (troilite, pyrrhotite, and mackinawite) or disulfide (iron pyrite and marcasite). They found in both soft (pyrrhotite) and hard (pyrite) form. Mono/di FeS/FeS_2 scales cause numerous operational issues in the oil and gas industry. They are found in a wide range of wells, viz., injector, manufacturer, removal, and supply wells, as both the iron and H_2S are present. The surface charge becomes more favorable due to the FeS/FeS_2 scales, and makes the rock more oil-wet, changing the relative permeability of the surface and decreasing the productivity of the surface. The sandstone rock contains iron ores. These scales have been removed from the reservoir rock; therefore, the efficiency of oil recovery enhanced by >20% [57,58].

3.1.2. Other Sulfide Scales

Besides iron sulfide scales, the uncommon sulfide scales of lead and zinc have also been reported by some researchers [51,56]. These scales are set down on the frontier side of the well, which produces a water control valve and, in the subsurface, produces safety control valves, respectively, and mainly

found in the wells of the area of the Gulf of Mexico and the North Sea. These scales are less soluble in water as compared to the iron sulfide scales. The solubility of these sulfide scales (Fe, Pb, and Zn) at different pH levels in 1 M NaCl solution is presented in Figure 1a. At the studied pH range (0–8), the solubility was the highest for iron sulfide scales compared to that of the other two (Pb and Zn). As an increase in the salinity and temperature, the solubility of the zinc and lead sulfide scales increases, which confirms that the cold salt-water leads to the scale formation of Zn and PbS. A well-known PbS scale, wurtzite, appeared in the Gulf of Mexico well. In the fields of the Gulf of Mexico, the literature reported the concentration of Zn^{2+} was found to be 245 ppm. These ions come from the ore of zinc, commonly known as sphalerite, in the injection/formation of brine. When zinc reacts with H_2S (2 ppm), it results in the deposition of the ZnS scale. It was shown that a loss of 500 bbl ZnBr within the reservoir could deposit zinc sulfide scales significantly, as it was reported that ZnBr was found to be a good source of Zn-ion. Besides this, the lead sulfide scales can be obtained from their primary sources from the partial dissolution of galena. The Pb^{2+} ion concentration in the well of the Gulf of Mexico was found to be around 70 ppm, as reported in the literature [59–62].

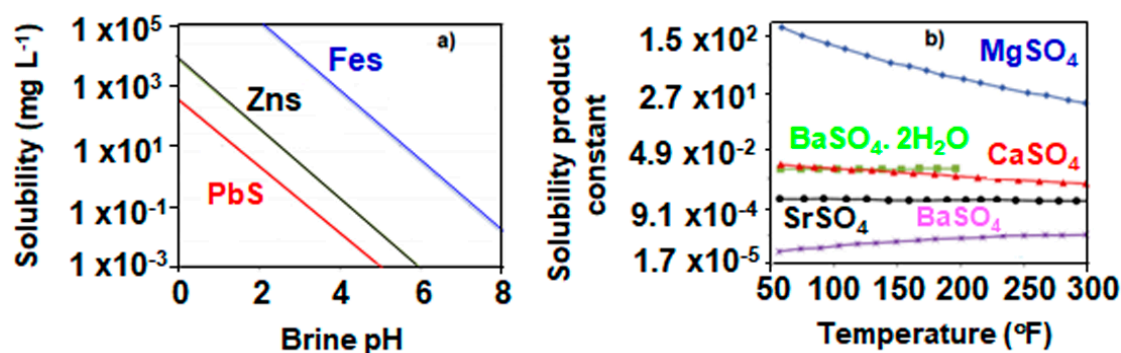


Figure 1. (a) Solubility vs. pH curves of different sulfide scales in 1 M NaCl at 25 °C. (b) Solubility of sulfate scale.

3.2. Sulfate Scales

These are some of the most challenging forms of scales, possessing low solubility in acids and difficult to remove in the seawater injection-related applications. Sulfate scales are formed due to the combination of two different kinds of water in which one consists of ions of alkaline metals, while others contain sulfate ions. Figure 1b describes the solubility product constant (K_{sp}) values for various alkaline metal ion based scales. The larger K_{sp} values correspond to the higher solubility in a particular solution. From Figure 1b, it can be seen that the K_{sp} value of gypsum is highest at all temperatures, where BaSO_4 has the lowest K_{sp} [63,64].

3.2.1. Barium Sulfate

BaSO_4 scales can be obtained from two primary sources in which one of them is the injection of seawater into the zone where the excess of Ba^{2+} ion dominates the deposition of BaSO_4 scales. The deposition of scales proceeds due to the excess SO_4^{2-} ions and excess of Ba^{2+} ions. Another process is the drilling operations resulting in the BaSO_4 scales deposition in the formation and the production tubing. BaSO_4 scale has the value of K_{sp} about $10^{-9.99}$ at 25 °C for the solubility of 2.3 mg L^{-1} of water, while for gypsum, K_{sp} is around the same at the same temperature for the solubility of 2080 mg L^{-1} [65,66].

3.2.2. Calcium Sulfate

CaSO_4 is considered as a significant scale that transpired in the oil and gas industry. A study by Al-Khaldi et al. confirms that CaSO_4 may cause considerable change in injector and producer reservoirs [67]. Mahmoud et al. demonstrated that the deposition of these scales in the reservoir

could change the porosity and permeability of the reservoir [68]. The study of Oddo et al. revealed the deposition of CaSO_4 scale around the electrical submersible pump in the reservoir. In this study, the CaSO_4 crystals were found in three forms as hydrous, hemihydrates, and anhydrite of gypsum; that is why its precipitation is complicated. The formation of gypsum usually is at low temperature. At the same time, the deposition of its anhydrite forms at high temperatures. As temperature increases, the solubility of scales is increased up to 40°C , and when $T > 40^\circ\text{C}$, the solubility of CaSO_4 decreases [69]. Several authors reported that the exact prediction for the formation and deposition of CaSO_4 scales is complicated in a particular condition. However, when the temperature is higher than 40°C , the solubility of gypsum appeared to be higher than that of anhydrite. Usually, CaSO_4 is less soluble at low pressures, and the solution contains high pH. The solubility of CaSO_4 can also be affected by the ionic strength of the solution. In general, by increasing the ionic strength, the solubility of the scale can be maximized [70,71].

3.3. Carbonate Scales

Within carbonate-based scales for all alkaline earth metal ions, the CaCO_3 scale is the most common and most widespread on the upper part of the production tubing and in topside production facilities. The plot of the K_{sp} values for various carbonate scales is described in Figure 2 [64]. The formation of carbonate scale depends on temperature, the concentration of Ca^{2+} , pH, the concentration of bicarbonate, and the ionic strength of the solution. From the plot (Figure 2), it can be seen that MgCO_3 scales have the highest K_{sp} at low temperatures, while SrCO_3 has the lowest K_{sp} value. There are various CaCO_3 scales such as calcite, aragonite, and vaterite, of which calcite is the most stable form of CaCO_3 scales. In the decomposition of CaCO_3 , an equilibrium exists between CO_2 and ions in the water that determines the deposition of CaCO_3 scale, and this deposition of scale can take place via a combined form of the ions of calcium and bicarbonates, respectively [72,73]. Several researchers reported that the deposition of carbonate scales is increased with an increase in pH, temperature, and a decrease in pressure. Transition metal carbonate scales, mostly iron-based, have also been reported in various downhill equipment. Siderite, an ore of iron and the chief source in the formation of scale, varies with changing the temperature and pressure, which leads to the loss of dissolved CO_2 . Various types of scales based on Ca^{2+} ion are phosphates, silicates, and the elemental sulfur in which phosphate scales are widespread in cooling water and water treatment plants. Phosphate scales are not very common in the oilfield. Other than phosphate scales, silicate scales are found during steam injection operations. Iron silicate scales were found in downstream processes in a siliceous reservoir as reported, which may cause the plugging and corrosion of the facilities of the surface. The formation of silicates scales has been found in the steam generator, which has been reported by several researchers. They confirm that the calcite scales were more dominant compared to silicate scales [74–76].

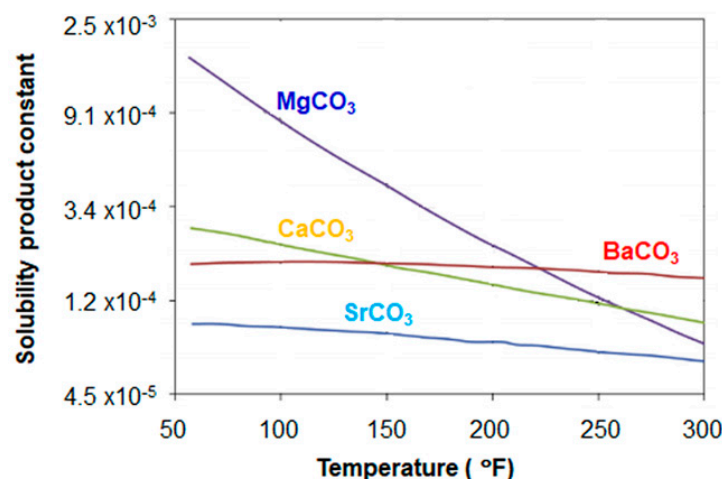


Figure 2. Solubility of carbonate scale.

4. Mechanism of Scale Inhibitions

The mechanism of scale inhibition primarily depends on the chemical nature of inhibitors. It could be held in various ways, such as sequestering (or chelating) or threshold scale inhibitors. The mechanisms of scale inhibition by chemical inhibitors as a function of the surface conditioner to inhibit the scale formation are discussed below:

4.1. Chelants (Sequestrants)

Organic/inorganic molecules having chelating properties are used as inhibitors to prevent scaling. Ethylenediaminetetraacetic acid (EDTA), diethylenetriamine pentaacetic acid (DTPA), citric acid, and gluconic acid are typical examples of chelants. The function of chelating agents by chelation is to prevent scale formation. The anionic part of the inhibitor combines with the cationic part like the metal ion in the solution, resulting in the forming of a coordinate bond with the scaling cation (*vide supra*, Figure 3) [77]. Depending on the combining stoichiometric ratio of cations and anions in the solution, the chelant molecules bond with scaling cations. However, the inhibition of the formation of scale by the use of chelating agents is expensive. On a large scale, the chemicals are needed for the successful prevention of scales as they are functioning in a stoichiometric fashion [5,77].

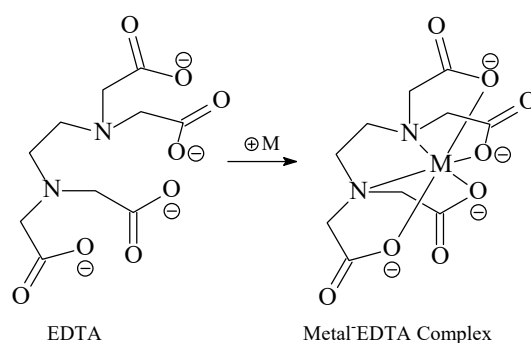


Figure 3. A representation of an ethylenediaminetetraacetic acid (EDTA) chelating molecule.

4.2. Threshold Scale Inhibitors

This type of inhibitors has been used to prevent scale precipitation by delaying the crystal growth of the mineral/ore. They prevent the corrosion or deposition of scale by interfering in a single or more than one step of the formation of scales. In general, the creation of scales includes several steps, such as crystal growth, nucleation, agglomeration, and/or intervening in aggregation. Mechanisms are accumulated to the function as primer or combinations of the distortion of the crystal, nucleation inhibition, and threshold inhibition and/or dispersion mechanisms. This type of mechanism is defined by adding a substoichiometric quantity of inhibitors that intermingles with growing crystals and delays crystal growth [78,79]. Several works on the threshold mechanism conducted by the number of researchers reveal that a scale inhibitor is conceived to intervene in the development of nucleation. They adsorbed onto the dynamic sites of the crystals and distorted the morphology of the crystals. Thus, the scale inhibitors prevented the crystalline lattice formation with their regular morphology and accumulation of adherent scales, and are called nucleation inhibitors. Polymeric organic and phosphinopolycarboxylic acid scale inhibitors mainly work as nucleation inhibitors under the threshold mechanism. It made the inhibition more effective, and during the stage of the nucleation process of growth of the crystal, the antiscalants should be present. The inhibitors inhibited the scale crystal from sticking to the surface and hindered a scale deposit [77,80–82].

4.3. Fluorescent-Tagged Scale Inhibitors

In a common perspective, the chemical inhibitors can control the scale deposition. However, the mechanism of CaCO_3 and CaSO_4 inhibition by the chemical process for

the long-term scale inhibition application despite everything remains a matter of further consideration [83]. Very recently, Oschepkov et al. proposed a mechanism of scale inhibition on CaSO_4 to locate and understand the presence of fluorescent tag scale inhibitors using a visualization study [84,85]. To better understand the new mechanism into the system of the scale formation and inhibition, a fluorescent-labeled bisphosphonate scale inhibitor 1-hydroxy-7-(6-methoxy-1,3-dioxo-1H-benzo[de] isoquinolin-2(3H)-yl)heptane-1,1-diyl-di(phosphonic corrosive), (HEDP-F) was synthesized and observed under a fluorescent microscope for CaSO_4 inhibition in a supersaturated aqueous solution [84]. The visualization of HEDP-F suggested a nonconventional mechanism of CaSO_4 scale inhibition, which is fundamentally not quite the same as the traditional ones. It showed that Ca^{2+} form complex with HEDP-F leads to the insoluble particles followed by a heterogeneous nucleation mechanism [86]. The insoluble particles do not stockpile yet remains as small strong particles dispersed in the fluid phase, and develop without noticeable sorption of bisphosphonate on the crystal edges or some other crystal development centers; subsequently, obstruct the CaSO_4 crystals dynamic development sites, and retard the formation of scale [87]. Later, the same research group studied a scale inhibition efficiency and fluorescent properties of another newly developed fluorescent antiscalant-1, 8-naphthalimide-tagged polyacrylate (PAA-F1) [85]. A similar outcome was acquired for PAA-F1 that was realized in the presence of HEDP-F for CaSO_4 RO desalination process [88], batch static tests with CaSO_4 [84] and barite [89], and supports the proposed mechanism.

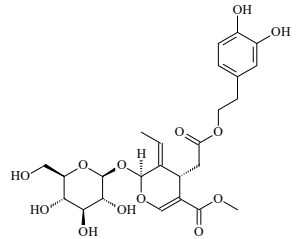
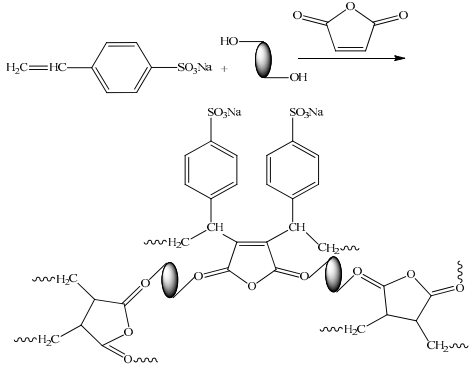
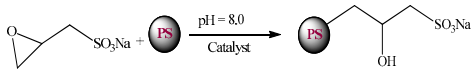
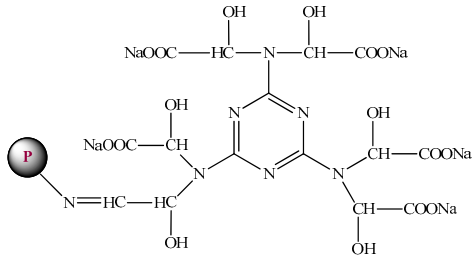
5. Scale Inhibitors

As discussed earlier in the introduction section, a corrosion or scale inhibitor is a chemical substance added in a low amounts to the brine to prevent or reduce the formation of scale. From various sources, we realized a “scale inhibitor” as a chemical compound that slows down the rate of scaling, retards, or prevents the mineral/ore scales are forming in brine saturated with oppositely charged scaling ions with the chelating scale ions. They typically consist of many active functional groups of similar or different types that have the capability to bind strongly or weakly with the cations of scales or with the forming nuclei or with the growing crystal, thereby holding them in aqueous solution. Inorganic- or organic-compound-based scale inhibitors can be used in oilfields systems to prevent or retard the formation of scale in the production conduit or completion system. Water-soluble organic (polymers) and inorganic (chelates) compounds having relatively low concentrations decrease the rate of the formation of scales in well production in the petroleum industry. Polymeric scale inhibitors derived from organic constituents are invaluable since they are usually classified as green scale inhibitors. The applications of green scale inhibitors do not truly hurt nature and demonstrated great dissolvability, permitting them to be unrivaled in forestalling scale deposition for supersaturated saline environments. Besides, organic polymeric scale inhibitors are relatively cheap as they are synthesized from inexpensive and readily available precursors and follow the straightforward and economical synthetic routes. Nowadays, a broad range of chemicals, natural, synthetic or semisynthetic, are well known, which can be applied as green antiscalants [81,90]. Some of them are discussed below.

5.1. Natural Organic Molecule

Abdel-Gaber et al. studied fig leaf extracts, which are economically beneficial and easily grow in highly calcareous soil conditions in the Mediterranean coastal zone. The study concluded that those extracts have the best quality to compile calcium, which constitutes a large mineral mass percentage in the aboveground parts of these plants [91]. The same research group further studied an olive leaf extract *Punica granatum* hull extract, and tested for scale inhibition [92,93]. Some other researchers [15,94] have used synthesized sulfonate using hetero-polysaccharide, corn stalks, and cheap raw materials, copolymer modified with palygorskite and carboxyl-rich collagen modifier for scale inhibition. The characteristic properties of these antiscalants are described in Table 2.

Table 2. Characteristics of antiscalant properties of some natural organic molecules.

Antiscalants	Schematic Structure	Dosages (mg L ⁻¹)	Performance (%IE)	Scalant	Ref.
Olive leaf extract (Biopheols)		50	83	CaCO ₃	[15]
Copolymer modified with the palygorskite		50	99	CaCO ₃	[15]
Heteropolysaccharide sulfonate (PS-NAEP)		100	95 55	CaSO ₄ Ca ₃ (PO ₄) ₂	[15]
Modification of collagen (P-MACs)		7	100	CaSO ₄	[94]

More studies have also been conducted using naturally occurring organic molecules to inhibit scale [14,15,95]. They are accepted as environmentally benign in comparison to conventional scale inhibitors. Scale inhibition for the crystal growth of CaCO_3 by xanthan molecules is a type of polysaccharide obtained from bacteria known as *Xanthomonas campestris* has been reported by Yang et al. [95]. This bacterium is used on a large scale in pharmaceuticals, food, and self-care. At pH = 9, the crystallization of CaCO_3 has been studied by xanthan ($100\text{--}1000\text{ mg L}^{-1}$) in which the initial concentration of Ca^{2+} and CO_3^{2-} ions in the solution was calculated to be 2664 and 2544 mg L^{-1} , respectively. The inhibitive properties were examined by XRD that showed CaCO_3 particles exhibited a calcite scale. It was found that the crystallization particles are stacked in the presence of xanthan. Also, with an increase in concentration, the degree of stacking of particles decreases. They proposed that the carboxyl groups present in xanthan molecules scattered the CaCO_3 particles, which prevents it from forming an aggregate [95]. A research group from Japan studied the effectiveness of naturally occurring carboxylic acids (maleic, malonic, tartaric, succinic, and citric acids) on the crystallization of CaCO_3 . The works were performed at room temperature in “synthetic” water that consists of initially Ca^{2+} and HCO_3^- ions with adjusted ionic strength and pH. The growth of CaCO_3 observed by the light-scattering method and change in transmitted light intensity could be due to the reduction of pH [96]. The growth of the reaction can be described by the reaction illustrated in Equation (3).



It can be seen in this study that the concentration of citric acid ($\approx 13\text{ mg L}^{-1}$) is quite useful at the total concentration of calcium ion of 800 mg L^{-1} . The growth in CaCO_3 appeared to be prevented with the adsorption of carboxylic acid. The study showed that the inhibition efficiency primarily depends on the variation of the carboxyl groups within the compound. However, the study also concluded that structural confirmation like acid conformations might play a significant role in the properties of scale inhibition.

Reddy et al. investigated the growth rate of calcite mineral in the presence of citric acid, a linear poly-carboxylic acid at pH 8.55 and room temperature using the constant composition technique [97]. They have demonstrated that citric acid only showed the rate of growth reduction in moderate calcite crystal at relatively higher concentrations (10 mg L^{-1}), and no rate of growth reduction was observed in lower concentration ($0.01\text{--}0.1\text{ mg L}^{-1}$) with a concentration of Ca^{2+} ions is about 76 mg L^{-1} . As compared to linear poly-carboxylic acid, using the same technique, a cyclic rigid poly-carboxylic acid, such as tetrahydrofuran-tetracarboxylic acid/or cyclopentanetetracarboxylic acid, was very efficient against corrosion or scaling. The vaterite (a polymorph of CaCO_3) mineral was utilized to study the scaling process [98]. The investigations have been performed in the presence of the organic molecule leucine at pH 8.5 and room temperature. The study suggested that there was no effect on the growth mechanism by leucine. In the continuation of this study, glutamic acid was used instead of leucine; similar results were obtained. In another work, Dalas et al. studied the crystal growth of calcite in the presence of cysteine-rich Mdm2 peptide, which has also been performed using the constant composition technique [99]. The research findings reported the development of calcite crystal, and the Mdm2 peptide can inhibit the scale formation. The adsorption of Mdm2 peptide could block the growth in the active sites at the surface of the calcite crystal. Significantly, the fragments of Mdm2 interact with Ca^{2+} ions in the surface of the calcite crystal with H-bond or with their terminal carboxyl groups. A derivative of glutamic acid known as pteroyl-L-glutamic acid (PGLU) has been taken by Kumar et al. to show the performance of scale inhibition and they reported that a 100% scale inhibition was obtained through jar tests with the concentration of PGLU about 120 mg L^{-1} at $70\text{ }^\circ\text{C}$ [77]. The tested synthetic waters served as the interpreter and were found in an offshore oilfield. The obtained water on a large scale contains a large quantity of Ca^{2+} and HCO_3^- [100]. However, at a higher temperature ($90\text{--}110\text{ }^\circ\text{C}$), a high PGLU concentration ($160\text{--}200\text{ mg L}^{-1}$) was required to prevent the formation of scale. The research groups finally concluded that PGLU could be a potential green scale inhibitor used in the downstream oil reservoir [77].

5.2. Biodegradable Polymers

Due to the increasingly environmental stringent regulations, the general trends of research and development in scale inhibitors markets are now focused on biodegradable and environmentally friendly polymers [101]. The synthetic polymer based on maleic anhydride is obtained from the dehydration of maleic acid, widely used in scale inhibition. The copolymers of these polymers were prepared from free radical polymerization using unsaturated monomers. The polymerization reaction occurs in the presence of some organic peroxide, e.g., benzoyl peroxide, di-tertbutyl peroxide, tertbutyl peroxy benzoate, tertbutylhydroperoxide, dicumyl peroxide, azobis(isobutyronitrile). Using this typical synthetic route, the researchers successfully synthesized a poly (maleic anhydride), copolymer, or synthetic terpolymer of maleic anhydride as a polymeric product [102–105]. For a similar study, Fukumoto et al. have also been reported the polymerization reaction, but their synthetic route is different as described (vide supra) [106]. They have carried out the polymerization reaction of maleic anhydride using its polymerizable monomers in aqueous solution in the presence of various inorganic peroxides to synthesize polymaleate based co and terpolymers. Moreover, polymers based on maleic acids can conventionally be synthesized by hydrolyzing corresponding maleic anhydride polymers. Some of the conventional synthetic polymers prepared in this route are currently under study for scale inhibition [106].

Green scale inhibitors demonstrated some advantageous properties: they have voluntary biodegradability, possess high efficiency, and are nontoxic [107]. In scale inhibition, poly(aspartic acid) (PASP) is considered a promising green scale inhibitor because of its performance and environmentally friendly properties. It is a biodegradable polymer having no phosphorus atom and showing excellent performance on sulfate and carbonate scales of Ca^{2+} . PASP can be widely produced by several methods in the presence or absence of a catalyst, which has been reported by many researchers [108–114]. Commonly, many processes are involved in the formation of polysuccinimide that can be hydrolyzed into salt or acid form. The thermal polycondensation of (+) and (–)-aspartic acid is used to synthesize the PASP. The polymerization of PASP has been synthesized in the presence or absence of H_3PO_4 catalyst at about 300 °C.

The mechanism for the polymerization reaction of PASP is shown in Figure 4. The researchers also reported the catalyst polymerization reaction of aspartic acid onto polysuccinimide (PSI). It was found that aspartic acid polymerizes and reaches high molecular weight more quickly than the uncatalyzed polymerization reaction. In this study, they discussed the synthetic route for the preparation of PASP through thermal polycondensation methods in which they used the anhydride of maleic acid and ammonium carbonate or its derivatives ammonium maleate salt. However, these methods are found to be more expansive and less energy efficient. Both processes proceed through the formation of PSI, which is then hydrolyzed into PASP. The PASP significantly reduces the CaCO_3 scale deposition in which the concentrations of PASP and Ca^{2+} ions are reported to be 4 mg L^{-1} and 14225 mg L^{-1} , respectively. The microscopic observation indicated the modification in crystal morphology of calcite by PASP, which led to vaterite formation. Euvrard et al. [115] have reported that a low level of electrochemical generation of CaCO_3 deposition on the surface of stainless steel was observed while the meager concentration of PASP was applied. By the action of PASP, the active site of deposition decreases the rate of growth of CaCO_3 crystals. The work has been performed by Liu et al. to show the effect of PASP on the efficiency of scale inhibition at 80 °C under static test conditions in mineral water containing Ca^{2+} ion concentrations of 253 mg L^{-1} , and they found the efficiency $\approx 80\%$, which confirms the better inhibition activity of PASP [114].

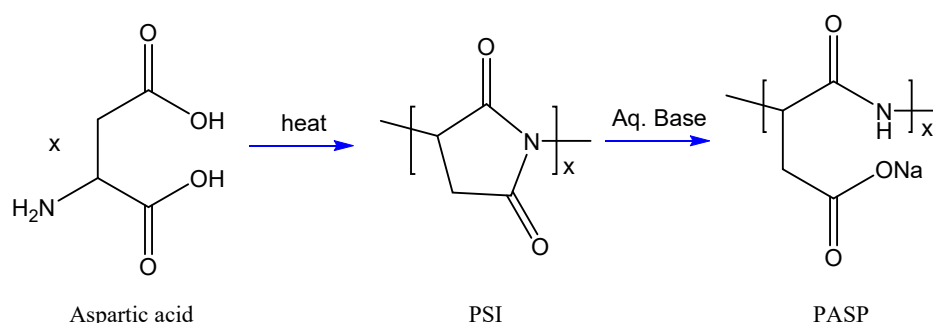


Figure 4. Typical synthetic route of poly (aspartic acid) (PASP) from aspartic acid.

5.3. Modified Natural Polymers

5.3.1. Chitosan and Substituted/Modified Chitosan

Chitosan bears hydroxyl and amino groups that have an excess of electrons and capable of binding the metal surface to subsequent scale inhibition through the coordinate bond in which electrons are coordinated to the empty or partially occupied metal orbitals to understand the antiscaling ability of chitosan. This polymer was utilized to study the inhibition efficiency at the metal surface in an acidic environment (HCl) and evaluated by various techniques such as SEM and FTIR. Literature reveals that chitosan can also be applied in the paper, textile, and food industries. The transplanting of these polar groups at the metal surface increased the total surface energy, thereby further aiding scale prevention [116–119]. The hydrophobic nature of chitosan that naturally occurs in chitin-rich exoskeletons of marine crustaceans has been used mostly against skin infections. It is used in drug-carriers in modern therapeutics and has fungal and antibacterial properties. The antibacterial functions of these compounds or their derivatives with different polymers have been explored for a scope of Gram-positive and –negative bacterial diseases. Besides this, the scale inhibition performance and structural properties of chitosan were studied by quantum chemical calculations [118]. The derivatives of chitosan with metal, like a mixture of carboxymethyl chitosan- Cu^{2+} , were investigated for scale prevention of mild steel in 1 M HCl at temperature ranges 298–353 K using gravimetric and electrochemical techniques [120]. Scale prevention on steel surfaces using carboxymethyl chitosan- Cu^{2+} showed synergistic effects since they were prevented by each element rather than the combined form.

5.3.2. Pectate

Pectic acid is also known as a polygalacturonic acid such as pectin, a type of natural polymer obtained from plants, but frequently occurring in ripened fruits. Its derivative, primarily pectates, are derived from the structural modification of pectin and/or pectic acids, which might be better foaming and emulsifying agents in different industries [121,122]. Pectates are the esters of pectic acid. Hromadkova et al. [123] have investigated the synthesis of a few pectates from citrus pectin through alkyl amidation followed by alkaline hydrolysis. In this study, they also tested the pectate amides for the foamability of their stabilizations. Schweiger et al. reported the synthesis of nitropectin by replacing the hydroxyl group of pectate, and studied its efficacy as a scale inhibitor [122]. With the different pectic materials, pectates have also participated in scale inhibition in few media in viewing for the utilization of their free alcoholic groups for bonding on the metal surface. In another study conducted by Zaafarany et al. [124] for scale inhibition of this modified natural polymer (pectates) as anionic polyelectrolytes in 4 M NaOH on the surface of Al metal using chemical methods. By weight loss measurements, they showed that, when pectate is present in the solution, the scale inhibition rate on the surface of Al metal and the magnitude of inhibition efficiency reached up to 88% for 1.6% pectate in the alkaline electrolyte solution. However, it is worthwhile to mention that, for scale inhibition, mostly, inhibition depends on the concentration of inhibitor and temperature. Notably, this study

lacks an explanation of the possible mechanism of scale prevention and/or kinetics/thermodynamic modeling. Without more in-depth research, this study suggested that the pectate has good potential for the inhibition of metal surface.

5.4. Scale Inhibitors Extracted from Natural Sources

Several works have been performed for green scale inhibition qualities of natural organic molecules from plant-derived extracts on static and dynamic levels, mainly in a research laboratory. Abdel-Gaber et al. first introduced the plant-derived extracts with economic benefits on a large scale that have grown well under calcareous soil conditions in the Mediterranean coastal zone. These trees have an excellent ability to accumulate a higher percentage of calcium and minerals [91–93]. The scale inhibition of CaCO_3 , which was performed with fig leaf extract, has been listed in Table 3.

Table 3. Schematic chemical structural constituents of plant-derived extracts as scale inhibitors.

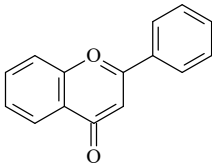
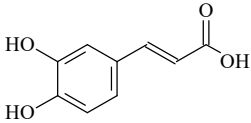
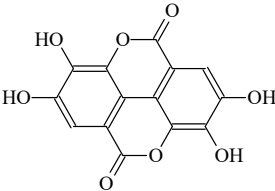
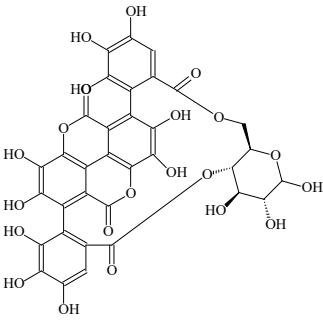
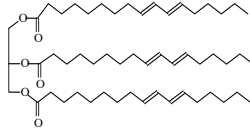
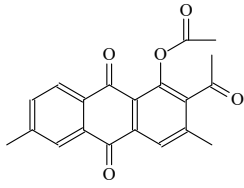
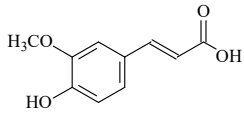
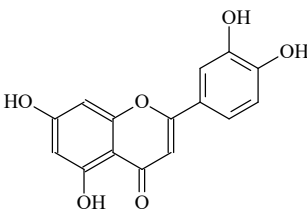
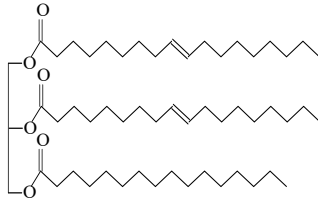
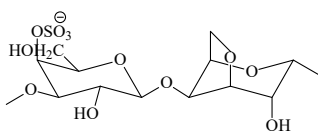
Antiscalants	Structure of Active Constituent	Dosages (mg L ⁻¹)	Performance (% IE)	Scalant	Ref.
<i>Ficus carica</i> L. (Fig) leaf extract	 Flavonoid	150	86	CaCO_3	[91]
<i>Olea europaea</i> L. (Olive) leaf extract	 Caffeic acid	50	83	CaCO_3	[92]
<i>Punica granatum</i> leaf extract	 Ellagic acid	100	60	CaCO_3	[93]
<i>Punica granatum</i> hull extract	 Punicalin	100	88	CaCO_3	[93]

Table 3. Cont.

Antiscalants	Structure of Active Constituent	Dosages (mg L ⁻¹)	Performance (% IE)	Scalant	Ref.
<i>Helianthus annuus seed extract</i>		50	100	CaSO ₄	[125]
		50	84	BaSO ₄	[125]
	Sunflower oil				
<i>Aloe vera extract gel</i>		15	80	CaCO ₃	[126]
	Anthraquinone				
<i>Paronychia argentea lam extract</i>		70	100	CaCO ₃	[127]
	Ferulic acid				
<i>Soybean-based polymer</i>		4250 3100	93 17	CaSO ₄ CaCO ₃	[128]
	Luteolin				
<i>Polysaccharide from seaweed</i>		4200 3100	90 17	CaSO ₄ CaCO ₃	[128]
	Soybean oil methyl ester				
<i>K-carrageenan</i>					

Chaussemier et al. prepared a stock solution after boiling ground fig leaves in boiling water and studied the scale inhibition for the deposition of CaCO₃ on a steel electrode by a chronoamperometry at 40 °C [129]. Using electrochemical impedance spectroscopy, the nucleation growth at the electrode surface was measured. Using such a stock solution (75 mg L⁻¹), it showed good inhibition efficiency of about 85%. Further, an optical microscopic study showed that even at a minimal concentration (5 mg L⁻¹), the extract of fig leaves could inhibit the coverage on the surface of the steel. The same research group has also investigated olive leaf extract in the place of fig leaf extract and prepared a stock solution using the same process. The olive leaves are rich in phenolic molecules (oleuropein), the most abundant biophenols in caffeic acid and olive leaves are as shown in Table 3. It was found that the olive leaf extracts could efficiently prevent the CaCO₃ scales. The scale inhibition performance for

the extract (polysaccharides and soybean) obtained from seaweeds have been demonstrated and found to follow the national association of corrosion engineers (NACE) standard [128]. The performance of scale inhibitors to inhibit the formation of CaCO_3 was evaluated through static laboratory tests. These works were performed in a brine solution at a meager concentration of (10 mg L^{-1}) inhibitor that contains Ca^{2+} ions of the initial concentration of 1215 mg L^{-1} at 71°C . The research groups predicted that these extracts could be more effective than polyaspartic acid to inhibit the formation of CaCO_3 . The inhibition efficiency was reported to be 16.7% for the extracts (polysaccharides and soybean) from seaweeds, while in the case of poly-aspartic acid, it was found only 6.6% [130–132]. From Table 3, we can also see that plants contain known compounds that form complexes with Ca^{2+} ions.

Abdel-Gaber et al. have made a further study on scale inhibition using *Punica granatum* hull and leaf extract for the scale inhibition of the CaCO_3 scale [93]. Their work revealed that the hull extract exhibited better scale inhibition activity than leaf extract. Moreover, it was also found that the leaf extracts can be used as effective antiscalants for the inhibition of mild steel in an acidic (H_2SO_4) environment. Aloe vera leaf extract was explored to study their inhibitive properties as an antiscalant for mild steel scale in $1 \text{ M H}_2\text{SO}_4$ using electrochemical and scanning electron microscopic techniques [133]. Their results provided useful information regarding leaf extract. Aloe vera (30% *v/v*) demonstrated maximum inhibition efficiency (98%). Hassan et al. studied *Citrus aurantium* leaf extracts for their antiscaling properties on mild steel scales in H_2SO_4 [134]. At a dose of 10 mL L^{-1} , the maximum inhibition efficiency was found to be 89%. Li et al. [135] performed a study considering *Osmanthus fragrance* leaves extract on carbon steel in 1 M HCl , and was demonstrated to be a mixed-type inhibitor. Orubite et al. investigated the performance of scale inhibition of extracts from leaves of *Nypa fruticans* plants on mild steel scale in HCl and compared them with the organic molecule 1,5-diphenylcarbazone. *Nypa fruticans* showed an inhibition efficiency of 75.11%, while the inhibition efficiency of 1,5-diphenylcarbazone was found to be only 70.18% [125].

5.5. Other Scale Inhibitors

5.5.1. Calcium Carbonate

Among the alkaline metal carbonate series, CaCO_3 is one of the most common scales framed because of the breakdown of HCO_3^- . The extent of scale inhibition initially relies on the hardness of Ca^{2+} ion and the basicity of bicarbonate of the source water. It showed that with an increase in the temperature and pH of the solution, the rate of the decomposition of the bicarbonate increases. The rate of decomposition may also affect total dissolve solids (TDS) content. In the literature, various forms of CaCO_3 and their hydrates, such as amorphous, monohydrated, and hexahydrated types, are discussed. Crystalline calcite, a kind of CaCO_3 , has well-organized rhombohedral arrangements with sharp and straight edges with an average particle size $\approx 10 \mu\text{m}$. In all three crystalline polymorphs, calcite is the most thermodynamically stable form of CaCO_3 . The amorphous form of CaCO_3 is thermodynamically unstable, feasible and spontaneous in a crystal form when presents in aqueous solution at ambient temperatures. The process of crystallization depends on a few factors (temperature, pH, and concentration) that lead to the formation of crystals. Aragonite or vaterite, also a form of CaCO_3 , is thermodynamically less stable than calcite. The antiscaling performance of calcite is more than that of the other states [126].

5.5.2. Calcium Sulfate

The sulfate scale of Ca^{2+} is a very common scale among the nonalkaline scales. It has also been found in various forms, such as calcium sulfate dehydrate (gypsum), calcium sulfate hemihydrates (plaster of Paris), and calcium sulfate anhydrite. Gypsum is the most common form of sulfate scale at ambient temperature. Many researchers have revealed via experimental investigations that two morphological structures of gypsum, needles and platelets with monoclinic and prismatic structures, are available [127,136]. Lash et al. [137] reported the needle morphology of gypsum that

is produced at room temperature from solutions and that initial concentrations of the needle type were >0.4 M in CaSO_4 whereas another type was less than 0.25 M in CaSO_4 . The investigations made by Christoffersen et al. [138], however, found this to be inverted as the low concentration favored the needle type (0.3 M CaSO_4). In contrast, the high concentration was made for platelet type (0.3 M CaSO_4). The crystalline morphology of gypsum has been seen to depend on crystallization kinetics and the supersaturating ratio. The crystal of the needle types was observed to be generated under conditions of a low supersaturation ratio of less than 2.27 . It prevailed by surface crystallization, and became distinguished over the induction period before the nucleation. Besides this, plate-like arrangements are observed with a supersaturation ratio of 10.86 , which dominates over bulk crystallization. These morphological structures of gypsum have been used as an antiscalant with their high inhibition efficiency.

5.5.3. Calcium Phosphate

Various crystalline forms of phosphate scales of calcium ion, such as fluorapatite and hydroxyapatite, have been found. These are the orthophosphate of calcium varying with the amount of OH^- , Cl^- , and F^- . The $\text{Ca}_3(\text{PO}_4)_2$ in crystalline apatite form was found to be less soluble in alkaline and neutral conditions and discriminatively dissolves in acidic pH. In contrast, the other form of phosphate (iron and aluminum) is less soluble at moderately alkaline conditions [139–141]. Based on the phosphate concentration, pHs and temperature, the stability index of $\text{Ca}_3(\text{PO}_4)_2$ was acquired [142], and this predicts the limit level of scale formation. Apart from CaCO_3 scale, there are no desirable antiscalants to alleviate $\text{Ca}_3(\text{PO}_4)_2$ scaling. Qin et al. [143] accomplished successful control of scale via the pH adjustment method. Commonly, the addition of antiscalants has less impact on the relief of the phosphate scale in comparison with pH adjustment approaches. Mainly, to control the pH of the feed water can effectively control the hazard of $\text{Ca}_3(\text{PO}_4)_2$ precipitation. This phenomenon has been investigated by Znini et al. [144] and described the advantage of the state to control the phosphate deposition. In this process, $\text{Ca}_3(\text{PO}_4)_2$ in its ionic forms breaks down to Ca^{2+} and orthophosphate ions, followed by the crystallization of $\text{Ca}_3(\text{PO}_4)_2$, which is more commonly held onto the film. Therefore, the efficacy of antiscalants becomes less effective. Thus, the following points might be considered to mitigate the risk of scale inhibition for $\text{Ca}_3(\text{PO}_4)_3$:

- (i) During pretreatment, the concentrations of orthophosphate, Ca, Al, Fe, and fluoride should be reduced.
- (ii) Dispersants can be used in the source when $\text{Ca}_3(\text{PO}_4)_3$ appears in the form of nanoparticles, and
- (iii) The reverse osmosis (RO) feed should be maintained at low pH.

In another way, if phosphate occurs in its colloidal form, the deposition of the colloid would be more likely to form on the film instead of crystallization and found to be the antiscalants are ineffective at its distinct levels of dosage. Therefore, anticoagulants are added to increase the activity of the antiscalants.

6. Comparative Performance Evaluation of Traditional and Green Scale Inhibitors

Every year new scale inhibitors are developed/synthesized and regularly tested on laboratory bench scale and pilot plants before using them in actual operational plants [145]. Scale inhibitors show enormous points of interest as they can smother scale arrangement with low doses (typically under 10 mg L^{-1}) and, thus, are considered cost-effective. The low dosages are a long way from the stoichiometric concentration of the scaling species.

The active ingredients in commercially available antiscalants are mostly proprietary mixtures of various polycarboxylates and polyacrylates, condensed polyphosphates, and organophosphonates [129,146]. Inorganic scale inhibitors, namely hexametaphosphate, poly(phosphate), pyrophosphate or phosphate esters, and phosphonates as organic phosphorus compounds, are profoundly flimsy in aqueous environments. Therefore, they usually hydrolyze, or react with water, and turn out to be an inefficient

orthophosphate [147]. Poly(phosphate) antiscalants have been, to a great extent, supplanted by different carboxylic-acid-based polymers (poly(acrylic acid), poly(maleic acid), etc.). They are steady at high working temperatures and stringent chemical and biological environments [148].

There is a particular concern about the phosphorus-based inhibitors, which can fill in as supplements prompting eutrophication difficulties [149]. Phosphorus and substantial metal releases are directed in various zones of the world, and passable cutoff points are diminishing. Chemicals released into the marine condition can potentially cause serious or long stretch effects on maritime living creatures. Regardless of whether these impacts are acknowledged relies upon various factors, for example, the natural harmfulness of the material, the amounts released and coming about fixations in the water section, the time allotment biota is presented to that focus, and the affectability of the organisms to specific chemicals [150].

Increasing environmental concerns lead to the synthesis of green antiscalants that show voluntary biodegradability for minimum environmental impact. Intensive efforts have been applied to develop new antiscalants, which are more stable, green and environmentally acceptable compared with conventional scale inhibitors. Some of them are reported in Table 4.

Table 4. List of some conventional and green scale inhibitors and their effectiveness as antiscalants.

Scale Inhibitors	Dosages (mg L ⁻¹)	Performance (% IE)	Scalant	Ref.
PBTC	12	91	CaCO ₃	[151]
HEDP	12	64	-	[151]
PEG ₈ DMA/AA	12	89	-	[151]
PESA	12	90	-	[114]
PASP	12	78	-	[114]
HPMA	20	37	-	[152]
PAA	20	29	-	[152]
AA-APEC	20	69	-	[152]
MA-APES	20	26	-	[152]
AA-APEL-PA	8	99	-	[153]
CM-QAOC	10	70	-	[154]
Cs-PASP	8	92	-	[155]
AA-APEC	8	96	-	[156]
Palm leaves extract	75	90	-	[157]
CG	15	91	-	[158]
Poly(carboxylic acid)	1	80	-	[97]
Poly(maleic acid)	10	56	-	[159]
Sodium alginate	0.02	94	-	[160]
PAA/APEG-PG-COOH	14	82	-	[153]
PBTC	4	60	CaSO ₄	[151]
HEDP	4	90	-	[151]
PEG ₈ DMA/AA	4	99	-	[151]
HPMA	2	79	-	[152]
PAA	2	38	-	[152]
AA-APEC	2	39	-	[152]
AA-APES	2	2	-	[152]
PESA	10	90	-	[161]
PASP	10	98	-	[161]
PAPEMP	3	79	-	[162]
Poly(citric acid)	25	99	-	[163]
AA-APEC	2	84	-	[162]
CG	10	95	-	[158]
PAP1	9	97	-	[164]
PAA/APEG-PG-COOH	3	100	-	[153]
PBTC	12	43	Ca ₃ (PO ₄) ₂	[152]
HEDP	12	32	-	[152]
PESA	12	34	-	[152]
HPMA	12	43	-	[152]
PAA	12	90	-	[152]
AA-APEC	12	98	-	[152]
MA-APES	12	88	-	[152]
PAA/APEG-PG-COOH	6	100	-	[153]

7. Significance of Green Scale Inhibitors

Scale inhibition of metals and alloys is an exciting and well-studied area of research to control scale formation in water treatment plants and the oil and gas industry based on various processes, such as reverse osmosis, multi-stage-flash, and other water treatment processes, such as cooling towers, boiler water, heat exchangers, evaporation plants, and oil and gas fields. However, every often lessening scale materialization in an oil well, water/air resistant assembly and transportation framework faces a huge challenge in the oil and gas industry. One of the most promising ways to control/reduce scale formation is the addition of small concentrations of the inhibitor to the system. Increasing environmental concerns and discharge regulations worldwide trigger the researcher to explore the green chemistry approach to synthesize environmentally benign and cost-effective green scale inhibitors.

Several green inhibitors have attracted considerable attention to the scientific community in the inhibition field due to their well-being, renewability, ecological acceptability, and biodegradability. These green inhibitors include amino acids, alkaloids, polyphenols, and often plant extracts that are enormously distributed and low economic value, including byproducts of agroindustrial processes and agricultural wastes. Many natural and synthesized organic compounds, which were used as antiscalants, are cheaper and are harmful to human health and the environment. The toxicity of these antiscalants should have a supporting path to investigate the utility of green antiscalants. They should be nontoxic, biodegradable, and environmentally friendly. Several works have been reported in the literature on developing green scale inhibitors [1–7,103–107]. Znini et al. [144] reported the environmentally friendly scale inhibitors for the scaling activity of steel in H_2SO_4 using purified compounds and essential oils, which can be achieved from plant extracts. El-Etre [165] have reported the effect of inhibition of the seeds of Khillah on scale inhibition of steel in HCl solution. The research group attributed the antiscaling performance of Khillah plant-derived extracts to the insoluble complexes formed from the interaction between Fe^{2+} ion and khillah extracts. Raja et al. [166] have reported some naturally occurring organic compounds, which are applicable as influential antiscalants. They observed that these naturally occurring compounds might serve as an excellent scale inhibitor with their usefulness, which comprises easy accessibility, nontoxicity, biodegradability, and eco-friendliness. Natural polymers such as cellulose, starch, and chitosan can be used for a desirable partial or complete alternative to synthetic polymers in specific applications by simple chemical modifications into hydrogels, flocculants, and slow-release encapsulating agents as well as starch phosphate. Despite many advantages of green scale inhibitors, the descaling and/or the removal of green scale inhibitors from the system sometimes incurred enormous difficulties. Jing and Tang examined the disadvantage and mechanism of the scale arrangement/expulsion and methods to take care of this issue comparable to the primary mechanism by which the inhibitors work [107]. Besides, the significant role of scale inhibitors are in RO processes, despite the more effective action of scale inhibition, few limitations surfaced by the use of scale inhibitors in RO operation are as follows:

- Optimal dosing of antiscalants is essential; otherwise, they can be a foulant as concentrations are high.
- Scale inhibitors are shown to increase the biofouling potential in RO systems. A few scale inhibitors can enhance the biological growth by up to 10 times.
- Pretreatment chemicals' carryover may react with scale inhibitors and form foulants or oppose the inhibition efficiencies. Using cationic flocculants for pretreatment can individually respond with few types of scale inhibitors forming sticky foulants.
- Polyacrylate shows a membrane type of foulant in the presence of Fe and other metal ions. Similarly, HEDP loses its efficiency of scale inhibition at high alkalinities and in the presence of chlorine.
- Observing the presence of scale inhibitors in the system is complicated, compared to evaluating the doses of acid by changing the pH.

8. Conclusions and Future Aspects

Scale formation is a typical phenomenon and generally encountered in aqueous systems when systems are supersaturated with salt ions. The formation of mineral scales influenced by the number of factors, such as temperature, pH, concentrations of salt ions, and pressure. Besides, the scaling potentials also depend on the application process, conditions, structure, and properties of scale inhibitors. This review article mainly discusses the following:

- Concept of scales;
- Different types of scales encountered in oil field reservoirs;
- Development of the scaling process on the surface;
- General mechanism of scale inhibitors;
- Environmentally benign green scale inhibitors (synthetic and natural source);
- Significance of scale inhibitors with a particular focus on green scale inhibitors.

Scale inhibition on an industrial scale, i.e., in oil and gas fields, is an onerous and long-term task that is vitally significant for oilfield development. That is why the scientific community has focused more attention on traditional scale inhibition technology and antiscalant discharge using chemical substances that contain nitrogen or phosphorus due to their higher stability towards biological, thermal, and chemical breakdown. Despite these advantages, their applications as scale inhibitors are limited due to the environmental consequences. They are usually toxic and nonbiodegradable. Moreover, the phosphorous and heavy metal discharges can serve as nutrients that lead to acute or long-term effects on aquatic organisms. These days, the water's eutrophic phenomenon becomes more serious. Processes of water reclamation, such as the desalination process, membrane filtration, and recirculating cooling water systems, are mostly used on industrial scale in settings where scales widely exist. These processes run in the long term by which the formation and deposition of scales remain an obstacle that decreases the heat transfer efficiencies, speeds up the membrane fouling, and even causes catastrophic accidents. Considering these constraints, the petroleum industry has been empowering the utilization of new classes of nontoxic substances dependent on nonphosphorus chemistry. Several works have been published during the last few years on natural and synthetic polymers and also on plant-derived extracts, which have shown a reasonably good performance towards scale inhibition, and even their inhibition efficiency was found to be very high. Scale inhibitors of alkaline earth metal carbonate and sulfates, transition metal sulfide like Fe, Zn, are commonly used in oilfield applications. Other than these, the renewable, biodegradable, relatively cheap, ecologically acceptable, and readily and sustainably available green scale inhibitors have been widely used to prevent, control, and retard the formation of scales. However, the biodegradability components of those green scale materials limit their enduring applications [167]. Still, there is a lot more to explore to find a scale inhibitor that exhibits acceptable biodegradable properties, is green, non-toxic, and cost-effective and does not pose any threat to the environment and the ecosystem. Scale inhibition technology of each oilfield should be linked with the situation to select and develop dedicated inhibition processes, which could be more efficient in the exploitation of oil and gas fields.

Funding: The author gratefully acknowledges King Fahd University of Petroleum & Minerals, KSA, for research and financial supports through project number CHEM2414.

Conflicts of Interest: The author declares no conflict of interest.

References

1. Bin Merdhan, A. Inhibition of calcium sulfate and strontium sulfate scale in waterflood. *SPE Prod. Oper.* **2010**, *25*, 545–552. [[CrossRef](#)]
2. Lu, H.; Kan, A.T.; Zhang, P.; Yu, J.; Fan, C.; Tomson, M.B. Phase stability and solubility of calcium sulfate in the system NaCl/monoethylene glycol/water. In Proceedings of the SPE International Conference on Oilfield Scale (SPE-130697-MS), Aberdeen, UK, 26–27 May 2010; pp. 1–26.

3. Zhang, Z.-J.; Lu, M.-L.; Liu, J.; Chen, H.-L.; Chen, Q.-L.; Wang, B. Fluorescent-tagged hyper-branched polyester for inhibition of CaSO_4 scale and the scale inhibition mechanism. *Mater. Today Commun.* **2020**, *25*, 101359. [\[CrossRef\]](#)
4. Jordan, M.M.; Williams, H.; Samaniego, S.L.; Frigo, D.M. New insights on the impact of high temperature conditions (176 °C) on carbonate and sulphate scale dissolver performance. In Proceedings of the SPE International Oilfield Scale Conference and Exhibition (SPE-169785-MS), Aberdeen, UK, 14–15 May 2014; pp. 1–17.
5. Olajire, A.A. A review of oilfield scale management technology for oil and gas production. *J. Pet. Sci. Eng.* **2015**, *135*, 723–737. [\[CrossRef\]](#)
6. Kan, A.; Tomson, M. Scale prediction for oil and gas production. *SPE J.* **2012**, *17*, 362–378. [\[CrossRef\]](#)
7. Yuan, X.; Dong, S.; Zheng, Q.; Yang, W.; Huang, T. Novel and efficient curcumin based fluorescent polymer for scale and corrosion inhibition. *Chem. Eng. J.* **2020**, *389*, 124296. [\[CrossRef\]](#)
8. Abd-El-Khalek, D.; Abd-El-Nabey, B. Evaluation of sodium hexametaphosphate as scale and corrosion inhibitor in cooling water using electrochemical techniques. *Desalination* **2013**, *311*, 227–233. [\[CrossRef\]](#)
9. Kamal, M.S.; Hussein, I.; Mahmoud, M.; Sultan, A.S.; Saad, M.A.S. Oil-field scale formation and chemical removal: A review. *J. Pet. Sci. Eng.* **2018**, *171*, 127–139. [\[CrossRef\]](#)
10. Qiang, X.; Sheng, Z.; Zhang, H. Study on scale inhibition performances and interaction mechanism of modified collagen. *Desalination* **2013**, *309*, 237–242. [\[CrossRef\]](#)
11. Yap, J.; Fuller, M.J.; Schafer, L.; Kelkar, S.K. Removing iron sulfide scale: A novel approach. In Proceedings of the Abu Dhabi International Petroleum Exhibition and Conference (SPE-138520-MS), Abu Dhabi, UAE, 1–4 November 2010.
12. Lakshmi, D.S.; Senthilmurugan, B.; Drioli, E.; Figoli, A. Application of ionic liquid polymeric microsphere in oilfield scale control process. *J. Petrol. Sci. Eng.* **2013**, *112*, 69–77. [\[CrossRef\]](#)
13. Balasubramanian, S.; Ghosh, B.; Sanker, S. High performance maleic acid based oil well scale inhibitors—Development and comparative evaluation. *J. Ind. Eng. Chem.* **2011**, *17*, 415–420. [\[CrossRef\]](#)
14. Antony, N.; Sherine, H.B.; Rajendran, S. Investigation of the inhibiting effect carboxymethylcellulose-Zn²⁺ system on the corrosion of carbon steel in neutral chloride solution. *Arab. J. Sci. Eng.* **2010**, *35*, 41–53.
15. Li, J.; Tang, M.-J.; Ye, Z.; Chen, L.; Zhou, Y.; Cheng, L. Scale formation and control in oil and gas fields: A review. *J. Dispers. Sci. Technol.* **2016**, *38*, 661–670. [\[CrossRef\]](#)
16. Kelland, M.A. *Production Chemicals for the Oil and Gas Industry*; CRC Press: Boca Raton, FL, USA, 2014.
17. Bader, M. Sulfate removal technologies for oilfields seawater injection operations. *J. Petrol. Sci. Eng.* **2007**, *55*, 93–110. [\[CrossRef\]](#)
18. Zhao, Y.; Xu, Z.; Wang, B.; He, J. Scale inhibition performance of sodium carboxymethyl cellulose on heat transfer surface at various temperatures: Experiments and molecular dynamics simulation. *Int. J. Heat Mass Transf.* **2019**, *141*, 457–463. [\[CrossRef\]](#)
19. Baugh, T.D.; Lee, J.; Winters, K.; Waters, J.; Wilcher, J. A fast and information-rich test method for scale inhibitor performance. In Proceedings of the Offshore Technology Conference (OTC 23150), Houston, TX, USA, 30 April–3 May 2012; pp. 1–10.
20. Huang, H.; Yao, Q.; Jiao, Q.; Liu, B.; Chen, H. Polyepoxysuccinic acid with hyper-branched structure as an environmentally friendly scale inhibitor and its scale inhibition mechanism. *J. Saudi Chem. Soc.* **2019**, *23*, 61–74. [\[CrossRef\]](#)
21. Ntourou, K.; DeFranco, E.O.; Conture, E.G.; Walden, T.A.; Mushtaq, N. A parent-report scale of behavioral inhibition: Validation and application to preschool-age children who do and do not stutter. *J. Fluency Disord.* **2020**, *63*, 105748. [\[CrossRef\]](#)
22. Yu, W.; Wang, Y.; Li, A.; Yang, H. Evaluation of the structural morphology of starch-graft-poly (acrylic acid) on its scale-inhibition efficiency. *Water Res.* **2018**, *141*, 86–95. [\[CrossRef\]](#)
23. Yang, Y.; Khan, F.; Thodi, P.; Abbassi, R. Corrosion induced failure analysis of subsea pipelines. *Reliab. Eng. Syst. Saf.* **2017**, *159*, 214–222. [\[CrossRef\]](#)
24. Li, X.; Chen, G.; Zhu, H. Quantitative risk analysis on leakage failure of submarine oil and gas pipelines using Bayesian network. *Process. Saf. Environ. Prot.* **2016**, *103*, 163–173. [\[CrossRef\]](#)

25. Alaoui, K.; Ouakki, M.; Abousalem, A.; Serrar, H.; Galai, M.; Derbali, S.; Nouneh, K.; Boukhris, S.; Touhami, M.E.; El Kacimi, Y. Molecular dynamics, Monte-Carlo simulations and atomic force microscopy to study the interfacial adsorption behavior of some triazepine carboxylate compounds as corrosion inhibitors in acid medium. *J. Bio Tribo Corros.* **2019**, *5*, 11–16. [\[CrossRef\]](#)
26. Alaoui, K.; Touir, R.; Galai, M.; Serrar, H.; Ouakki, M.; Kaya, S.; Tuzun, B.; Boukhris, S.; Touhami, M.E.; El Kacimi, Y. Electrochemical and computational studies of some triazepine carboxylate compounds as acid corrosion inhibitors for mild steel. *J. Bio Tribo Corros.* **2018**, *4*, 1–18. [\[CrossRef\]](#)
27. Majeed, N. Polymeric materials for scale inhibition in cooling water systems. *Tikritj. Eng. Sci.* **2011**, *18*, 1–11.
28. Popov, K.; Oshchepkov, M.; Afanas'Eva, E.; Koltinova, E.; Dikareva, Y.; Rönkkömäki, H. A new insight into the mechanism of the scale inhibition: DLS study of gypsum nucleation in presence of phosphonates using nanosilver dispersion as an internal light scattering intensity reference. *Colloids Surf. A Physicochem. Eng. Asp.* **2019**, *560*, 122–129. [\[CrossRef\]](#)
29. Amjad, Z.; Zuhl, R.W. The use of polymers to improve control of calcium phosphonate and calcium carbonate in high stressed cooling water systems. *Analysts* **2011**, *13*, 1–4.
30. Amjad, Z.; Landgraf, R.; Penn, J. Calcium sulfate dihydrate (gypsum) scale inhibition by PAA, PAPEMP, and PAA/PAPEMP blend. *Int. J. Corros. Scale Inhib.* **2014**, *3*, 35–47. [\[CrossRef\]](#)
31. Wang, C.; Li, S.-P.; Li, T.-D. Calcium carbonate inhibition by a phosphonate-terminated poly(maleic-co-sulfonate) polymeric inhibitor. *Desalination* **2009**, *249*, 1–4. [\[CrossRef\]](#)
32. Ansari, S.Z.; Pandit, A.B. Inhibition of Gypsum Scales on MS metal surface using hydrodynamic forces. *Chem. Eng. Process. Process. Intensif.* **2020**, *147*, 107706. [\[CrossRef\]](#)
33. Sanni, O.S.; Bukuaghangin, O.; Charpentier, T.V.; Neville, A. Evaluation of laboratory techniques for assessing scale inhibition efficiency. *J. Pet. Sci. Eng.* **2019**, *182*, 106347. [\[CrossRef\]](#)
34. Zhang, S.; Qu, H.; Yang, Z.; Fu, C.-E.; Tian, Z.; Yang, W. Scale inhibition performance and mechanism of sulfamic/amino acids modified polyaspartic acid against calcium sulfate. *Desalination* **2017**, *419*, 152–159. [\[CrossRef\]](#)
35. Fu, L.; Lv, J.; Zhou, L.; Li, Z.; Tang, M.; Li, J. Study on corrosion and scale inhibition mechanism of polyaspartic acid grafted β -cyclodextrin. *Mater. Lett.* **2020**, *264*, 127276. [\[CrossRef\]](#)
36. Miles, A.F.; Bourne, H.M.; Smith, R.G.; Collins, I.R. Development of a novel water in oil microemulsion based scale inhibitor delivery system. In Proceedings of the SPE International Symposium on Oilfield Scale (SPE 80390), Aberdeen, UK, 29–30 January 2003.
37. Zhang, D.-Q.; An, Z.-X.; Pan, Q.-Y.; Gao, L.-X.; Zhou, G.-D. Comparative study of bis-piperidiniummethyl-urea and mono-piperidiniummethyl-urea as volatile corrosion inhibitors for mild steel. *Corros. Sci.* **2006**, *48*, 1437–1448. [\[CrossRef\]](#)
38. Jordan, M.M.; Kramer, T.E.; Barbin, D.; Linares-Samaniego, S.; Arnette, W. Scale inhibitor squeeze treatments selection, deployed and monitoring in a deepwater Gulf of Mexico oilfield. In Proceedings of the SPE Annual Technical Conference and Exhibition (SPE 146400), Denver, CO, USA, 30 October–2 November 2011.
39. Vazquez, O.; Mackay, E.J.; Al Shuaili, K.H.; Sorbie, K.; Jordan, M.M. Modelling a surfactant preflush with non-aqueous and aqueous scale inhibitor squeeze treatments. In Proceedings of the EUROPEC/EAGE Conference and Exhibition (SPE 113212), Rome, Italy, 9–12 June 2008.
40. Jain, T.; Sanchez, E.; Owens-Bennett, E.; Trussell, R.; Walker, S.L.; Liu, H. Impacts of antiscalants on the formation of calcium solids: Implication on scaling potential of desalination concentrate. *Environ. Sci. Water Res. Technol.* **2019**, *5*, 1285–1294. [\[CrossRef\]](#)
41. Gan, T.; Zhang, Y.; Yang, M.; Hu, H.; Huang, Z.; Feng, Z.; Chen, D.; Chen, C.; Liang, J. Synthesis, characterization and application of a multifunctional cellulose derivative as an environmentally friendly corrosion and scale inhibitor in simulated cooling water systems. *Ind. Eng. Chem. Res.* **2018**, *57*, 10786–10797. [\[CrossRef\]](#)
42. Zhang, S.; Jiang, X.; Cheng, S.; Fu, C.; Tian, Z.; Yang, Z.; Yang, W.; Weiben, Y. Enhanced scale inhibition against $\text{Ca}_3(\text{PO}_4)_2$ and Fe_2O_3 in water using multi-functional fluorescently-tagged antibacterial scale inhibitors. *Environ. Sci. Water Res. Technol.* **2020**, *6*, 951–962. [\[CrossRef\]](#)
43. Peng, R.; Chen, G.; Zhou, F.; Man, R.; Huang, J. Catalyst-free synthesis of triazine-based porous organic polymers for Hg^{2+} adsorptive removal from aqueous solution. *Chem. Eng. J.* **2019**, *371*, 260–266. [\[CrossRef\]](#)
44. Malcolm, K. Effect of various cations on the formation of calcium carbonate and barium sulfate scale with and without scale inhibitors. *Ind. Eng. Chem. Res.* **2011**, *50*, 5852–5861.

45. Li, J.; Zhou, Y.; Yao, Q.; Wang, T.; Zhang, A.; Chen, Y.; Wu, W.; Sun, W. Preparation and evaluation of a polyether-based polycarboxylate as a kind of inhibitor for water systems. *Ind. Eng. Chem. Res.* **2017**, *56*, 2624–2633. [[CrossRef](#)]
46. Liu, G.; Xue, M.; Yang, H. Polyether copolymer as an environmentally friendly scale and corrosion inhibitor in seawater. *Desalination* **2017**, *419*, 133–140. [[CrossRef](#)]
47. Hoang, T.A.; Ang, H.M.; Rohl, A.L. Effects of temperature on the scaling of calcium sulphate in pipes. *Powder Technol.* **2007**, *179*, 31–37. [[CrossRef](#)]
48. Dayarathne, H.; Jeong, S.; Jang, A. Chemical-free scale inhibition method for seawater reverse osmosis membrane process: Air micro-nano bubbles. *Desalination* **2019**, *461*, 1–9. [[CrossRef](#)]
49. Herz, A.; Malayeri, M.; Müller-Steinhagen, H. Fouling of roughened stainless steel surfaces during convective heat transfer to aqueous solutions. *Energy Convers. Manag.* **2008**, *49*, 3381–3386. [[CrossRef](#)]
50. Hoang, T.A. Mechanisms of scale formation and inhibition. In *Mineral Scales and Deposits*, 1st ed.; Amjad, Z., Demadis, K.D., Eds.; Elsevier: Cambridge, MA, USA, 2015; pp. 47–83.
51. Berry, S.L.; Boles, J.L.; Singh, A.K.; Hashim, I. Enhancing production by removing zinc sulfide scale from an offshore well: A case history. *SPE Prod. Oper.* **2012**, *27*, 318–326. [[CrossRef](#)]
52. Mohammadi, Z.; Rahsepar, M. The use of green Bistorta Officinalis extract for effective inhibition of corrosion and scale formation problems in cooling water system. *J. Alloys Compd.* **2019**, *770*, 669–678. [[CrossRef](#)]
53. Tan, H.; Skinner, W.M.; Addai-Mensah, J. pH-mediated interfacial chemistry and particle interactions in aqueous chlorite dispersions. *Chem. Eng. Res. Des.* **2013**, *91*, 448–456. [[CrossRef](#)]
54. Zeino, A.; Albakri, M.; Khaled, M.; Zarzour, M. Comparative study of the synergistic effect of ATMP and DTPMPA on CaSO₄ scale inhibition and evaluation of induction time effect. *J. Water Process. Eng.* **2018**, *21*, 1–8. [[CrossRef](#)]
55. Yang, L.; Yang, W.; Xu, B.; Yin, X.; Chen, Y.; Liu, Y.; Ji, Y.; Huan, Y. Synthesis and scale inhibition performance of a novel environmental-friendly and hydrophilic terpolymer inhibitor. *Desalination* **2017**, *416*, 166–174. [[CrossRef](#)]
56. Ma, J.; Fuss, T.; Shi, J. Iron sulfide scale deposition in deep sour reservoirs. In Proceedings of the SPE International Conference and Exhibition on Formation Damage Control (SPE), Louisiana, LA, USA, 24–26 February 2016.
57. Mahmoud, M. Effect of chlorite clay mineral dissolution on the improved oil recovery from sandstone rocks during DTPA chelating agent flooding. *SPE J.* **2018**, *23*, 1–19. [[CrossRef](#)]
58. Bageri, B.S.; Mahmoud, M.; Abdulraheem, A.; Al-Mutairi, S.; Elkatatny, S.; Shawabkeh, R.A. Single stage filter cake removal of barite weighted water based drilling fluid. *J. Pet. Sci. Eng.* **2017**, *149*, 476–484. [[CrossRef](#)]
59. Al-Harbi, B.G.; Graham, A.J.; Sorbie, K. Zinc and lead interactions in combined sulphide scales. In Proceedings of the SPE International Conference on Oilfield Chemistry (SPE-184509-MS), Montgomery, TX, USA, 3–5 April 2017.
60. Baraka-Lokmane, S.; Hurtevent, C.; Rossiter, M.; Bryce, F.; Lepoivre, F.; Marais, A.; Tillement, O.; Simpson, C.; Graham, G.M. Design and performance of novel sulphide nanoparticle scale inhibitors for North Sea HP/Hatfields. In Proceedings of the SPE International Oilfield Scale Conference and Exhibition (SPE-179866-MS), Aberdeen, UK, 11–12 May 2016.
61. Lopez, T.H.; Yuan, M.; Williamson, D.A.; Przybylinski, J.L. Comparing efficacy of scale inhibitors for inhibition of zinc sulfide and lead sulfide scales. In Proceedings of the SPE International Symposium on Oilfield Scale (SPE-95097-MS), Aberdeen, UK, 11–12 May 2005.
62. Collins, I.; Jordán, M. Occurrence, prediction, and prevention of zinc sulfide scale within Gulf Coast and North Sea high-temperature and high-salinity fields. *SPE Prod. Facil.* **2003**, *18*, 200–209. [[CrossRef](#)]
63. Chilingar, G.V.; Mourhatch, R.; Al-Qahtani, G.D. *The Fundamentals of Corrosion and Scaling for Petroleum and Environmental Engineers*; Elsevier Science: Houston, TX, USA, 2013; ISBN 780127999913.
64. Li, Y.H.; Crane, S.D.; Coleman, J.R. A novel approach to predict the co-precipitation of BaSO₄ and SrSO₄. In Proceedings of the SPE Production Operations Symposium (SPE-29489-MS), Oklahoma, OK, USA, 2–4 April 1995.
65. Kuwahara, Y. In Situ atomic force microscopy study of dissolution of the barite (001) surface in water at 30 °C. *Geochim. Cosmochim. Acta* **2011**, *75*, 41–51. [[CrossRef](#)]

66. Bageri, B.; Mahmoud, M.; Shawabkeh, R.; Al-Mutairi, S.; Abdulraheem, A. Toward a complete removal of barite (barium sulfate BaSO_4) scale using chelating agents and catalysts. *Arab. J. Sci. Eng.* **2017**, *42*, 1667–1674. [\[CrossRef\]](#)
67. Al-Khaldi, M.H.; Aljuhani, A.; Al-Mutairi, S.H.; Gurmen, M.N. New insights into the removal of calcium sulfate scale. In Proceedings of the SPE European Formation Damage Conference (SPE-144158-MS), Noordwijk, The Netherlands, 7–10 June 2011.
68. Mahmoud, M. Effect of elemental-sulfur deposition on the rock petrophysical properties in sour-gas reservoirs. *SPE J.* **2014**, *19*, 703–715. [\[CrossRef\]](#)
69. Oddo, J.; Smith, J.; Tomson, M. Analysis of and solutions to the CaCO_3 and CaSO_4 scaling problems encountered in wells offshore Indonesia. In Proceedings of the SPE Annual Technical Conference and Exhibition (SPE-22782-MS), Dallas, TX, USA, 6–9 October 1991.
70. Moghadasi, J.; Müller-Steinhagen, H.; Jamialahmadi, M.; Sharif, A. Model study on the kinetics of oilfield formation damage due to salt precipitation from injection. *J. Petrol. Sci. Eng.* **2004**, *43*, 201–217. [\[CrossRef\]](#)
71. DeLorey, J.; Allen, S.; McMaster, L. Precipitation of calcium sulphate during carbonate acidizing: Minimizing the risk. In Proceedings of the Annual Technical Meeting (Petro-96-84), Calgary, AB, Canada, 10–12 June 1996. [\[CrossRef\]](#)
72. Amiri, M.; Moghadasi, J.; Jamialahmadi, M. Prediction of iron carbonate scale formation in Iranian oilfields at different mixing ratio of injection water with formation water. *Energy Sources Part A Recover. Util. Environ. Eff.* **2013**, *35*, 1256–1265. [\[CrossRef\]](#)
73. Zhao, Y.; Chen, Z.; Yang, F.; Zhen, Y. Ionic Liquid: A Promising Material for Petroleum Production and Processing. *Curr. Org. Chem.* **2020**, in press. [\[CrossRef\]](#)
74. Hamid, S.; De Jesus, O.; Jacinto, C.; Izetti, R.; Pinto, H.; Droguett, E.L.; Edwards, C.; Cassidy, J.; Zhang, H.; Dagenais, P.; et al. A practical method of predicting calcium carbonate scale formation in well completions. *SPE Prod. Oper.* **2016**, *31*, 1–11. [\[CrossRef\]](#)
75. Ramstad, K.; Tydal, T.; Askvik, K.M.; Fotland, P. Predicting carbonate scale in oil producers from high temperature reservoirs. *SPE J.* **2005**, *10*, 363–373. [\[CrossRef\]](#)
76. Wang, W.; Wei, W. Silica and silicate scale formation and control: Scale modeling, lab testing, scale characterization and field observation. In Proceedings of the SPE International Oilfield Scale Conference and Exhibition (SPE-179897-MS), Aberdeen, UK, 11–12 May 2016.
77. Kumar, S.; Naiya, T.K.; Kumar, T. Developments in oilfield scale handling towards green technology-A review. *J. Pet. Sci. Eng.* **2018**, *169*, 428–444. [\[CrossRef\]](#)
78. Abdel-Aal, N.; Sawada, K. Inhibition of adhesion and precipitation of CaCO_3 by aminopolyphosphonate. *J. Cryst. Growth* **2003**, *256*, 188–200. [\[CrossRef\]](#)
79. Issabayev, Y.A.; Boiko, G.I.; Lyubchenko, N.P.; Shaikhutdinov, Y.M.; Muhr, H.; Colombeau, L. Synthesis of unexplored amino phosphonic acid and evaluation as scale inhibitor for industrial water applications. *J. Water Process. Eng.* **2018**, *22*, 192–202. [\[CrossRef\]](#)
80. Sorbie, K.; Mackay, E.J. Mixing of injected, connate and aquifer brines in waterflooding and its relevance to oilfield scaling. *J. Pet. Sci. Eng.* **2000**, *27*, 85–106. [\[CrossRef\]](#)
81. Tomson, M.; Fu, G.; Watson, M.; Kan, A. Mechanisms of mineral scale inhibition. *SPE Prod. Facil.* **2003**, *18*, 192–199. [\[CrossRef\]](#)
82. Zhang, P.; Shen, D.; Kan, A.T.; Tomson, M.B. Phosphino-polycarboxylic acid-modified inhibitor nanomaterial for oilfield scale control: Transport and inhibitor return information media. *RSC Adv.* **2016**, *6*, 59195–59205. [\[CrossRef\]](#)
83. Popov, K.I.; Oshchepkov, M.S.; Shabanova, N.A.; Dikareva, Y.M.; Larchenko, V.E.; Koltinova, E.Y. DLS study of a phosphonate induced gypsum scale inhibition mechanism using indifferent nanodispersions as the standards for light scattering intensity comparison. *Int. J. Corros. Scale Inhib.* **2018**, *7*, 9–24.
84. Oshchepkov, M.S.; Kamagurov, S.; Tkachenko, S.; Ryabova, A.; Popov, K. Insight into the mechanisms of scale inhibition: A case study of a task-specific fluorescent-tagged scale inhibitor location on Gypsum crystals. *ChemNanoMat* **2019**, *5*, 586–592. [\[CrossRef\]](#)
85. Oshchepkov, M.; Golovesov, V.; Ryabova, A.; Redchuk, A.; Tkachenko, S.; Pervov, A.G.; Popov, K. Gypsum crystallization during reverse osmosis desalination of water with high sulfate content in presence of a novel fluorescent-tagged polyacrylate. *Crystals* **2020**, *10*, 309. [\[CrossRef\]](#)

86. Mbogoro, M.M.; Peruffo, M.; Adobes-Vidal, M.; Field, E.L.; O'Connell, M.A.; Unwin, P.R. Quantitative 3D visualization of the growth of individual Gypsum microcrystals: Effect of $\text{Ca}_2^+:\text{SO}_4^{2-}$ ratio on kinetics and crystal morphology. *J. Phys. Chem. C* **2017**, *121*, 12726–12734. [\[CrossRef\]](#)
87. Dobberschütz, S.; Nielsen, M.R.; Sand, K.K.; Civioc, R.; Bovet, N.; Stipp, S.L.S.; Andersson, M.P. The mechanisms of crystal growth inhibition by organic and inorganic inhibitors. *Nat. Commun.* **2018**, *9*, 1578. [\[CrossRef\]](#)
88. Oshchepkov, M.; Golovesov, V.; Ryabova, A.; Tkachenko, S.; Redchuk, A.; Rönkkömäki, H.; Rudakova, G.; Pervov, A.; Popov, K. Visualization of a novel fluorescent-tagged bisphosphonate behavior during reverse osmosis desalination of water with high sulfate content. *Sep. Purif. Technol.* **2020**, 117382. [\[CrossRef\]](#)
89. Oshchepkov, M.; Popov, K.; Ryabova, A.; Redchuk, A.; Tkachenko, S.; Dikareva, J.; Koltinova, E. Barite crystallization in presence of novel fluorescent-tagged antiscalants. *Int. J. Corros. Scale Inhib.* **2019**, *8*, 998–1021.
90. Sorbie, K.S.; Laing, N. How scale inhibitors work: Mechanisms of selected barium sulphate scale inhibitors across a wide temperature range. In Proceedings of the SPE International Symposium on Oilfield Scale (SPE-87470-MS), Aberdeen, UK, 26–27 May 2004.
91. Abdel-Gaber, A.M.; Abd-El-Nabey, B.A.; Khamis, E.; Abd-El-Khalek, D.E. Investigation of fig leaf extract as a novel environmentally friendly antiscalant for CaCO_3 calcareous deposits. *Desalination* **2008**, *230*, 314–328. [\[CrossRef\]](#)
92. Abdel-Gaber, A.; Abd-El-Nabey, B.; Khamis, E.; Abd-El-Khalek, D. A natural extract as scale and corrosion inhibitor for steel surface in brine solution. *Desalination* **2011**, *278*, 337–342. [\[CrossRef\]](#)
93. Abdel-Gaber, A.M.; Abd-El-Nabey, B.A.; Khamis, E.; Abd-El-Khalek, D.E.; Aglan, H.; Ludwick, A. Green antiscalant for cooling water systems. *Int. J. Electrochem. Sci.* **2012**, *7*, 11930–11940.
94. Al-Sabagh, A.; El Basiony, N.; Sadeek, S.; Migahed, M. Scale and corrosion inhibition performance of the newly synthesized anionic surfactant in desalination plants: Experimental, and theoretical investigations. *Desalination* **2018**, *437*, 45–58. [\[CrossRef\]](#)
95. Yang, X.; Xu, G. The influence of xanthan on the crystallization of calcium carbonate. *J. Cryst. Growth* **2011**, *314*, 231–238. [\[CrossRef\]](#)
96. Wada, N.; Kanamura, K.; Umegaki, T. Effects of carboxylic acids on the crystallization of calcium carbonate. *J. Colloid Interface Sci.* **2001**, *233*, 65–72. [\[CrossRef\]](#)
97. Reddy, M.M.; Hoch, A.R. Calcite crystal growth rate inhibition by polycarboxylic acids. *J. Colloid Interface Sci.* **2001**, *235*, 365–370. [\[CrossRef\]](#)
98. Malkaj, P.; Kanakis, J.; Dalas, E.; Kanakis, I. The effect of leucine on the crystal growth of calcium carbonate. *J. Cryst. Growth* **2004**, *266*, 533–538. [\[CrossRef\]](#)
99. Dalas, E.; Chalias, A.; Gatos, D.; Barlos, K. The inhibition of calcium carbonate crystal growth by the cysteine-rich Mdm2 peptide. *J. Colloid Interface Sci.* **2006**, *300*, 536–542. [\[CrossRef\]](#)
100. Zhu, T.; Wang, L.; Sun, W.; Wang, M.; Tian, J.; Yang, Z.; Wang, S.; Xia, L.; He, S.; Zhou, Y.; et al. The role of corrosion inhibition in the mitigation of CaCO_3 scaling on steel surface. *Corros. Sci.* **2018**, *140*, 182–195. [\[CrossRef\]](#)
101. Popov, K.; Kovaleva, N.E.; Rudakova, G.Y.; Kombarova, S.P.; Larchenko, V.E. Recent state-of-the-art of biodegradable scale inhibitors for cooling-water treatment applications (Review). *Therm. Eng.* **2016**, *63*, 122–129. [\[CrossRef\]](#)
102. Davies, M.C.; Dawkins, J.V.; Hourston, D. Radical copolymerization of maleic anhydride and substituted styrenes by reversible addition-fragmentation chain transfer (RAFT) polymerization. *Polymer* **2005**, *46*, 1739–1753. [\[CrossRef\]](#)
103. Sugama, T. Oxidized potato-starch films as primer coatings of aluminum. *J. Mater. Sci.* **1997**, *3*, 3995–4003. [\[CrossRef\]](#)
104. Nasirtabrizi, M.H.; Ziaei, Z.M.; Jadid, A.P.; Fatin, L.Z. Synthesis and chemical modification of maleic anhydride copolymers with phthalimide groups. *Int. J. Ind. Chem.* **2013**, *4*, 11. [\[CrossRef\]](#)
105. Von Bonin, W. Maleic Acid Anhydride Copolymers and Their Preparation. U.S. Patent 4,390,672, 1983.
106. Fukumoto, Y.; Moriyama, M. Production of Polymaleic Acid. U.S. Patent 4,709,091, 24 November 1987.
107. Jing, G.; Tang, S. The summary of the scale and the methods to inhibit and remove scale formation in the oil well and the gathering line. *Recent Patents Chem. Eng.* **2011**, *4*, 291–296. [\[CrossRef\]](#)

108. Ajikumar, P.K.; Low, B.J.M.; Valiyaveetil, S. Role of soluble polymers on the preparation of functional thin films of calcium carbonate. *Surf. Coat. Technol.* **2005**, *198*, 227–230. [\[CrossRef\]](#)
109. Migahed, M.; Rashwan, S.; Kamel, M.M.; Habib, R. Synthesis, characterization of polyaspartic acid-glycine adduct and evaluation of their performance as scale and corrosion inhibitor in desalination water plants. *J. Mol. Liq.* **2016**, *224*, 849–858. [\[CrossRef\]](#)
110. Quan, Z.; Chen, Y.; Wang, X.; Shi, C.; Liu, Y.; Ma, C. Experimental study on scale inhibition performance of a green scale inhibitor polyaspartic acid. *Sci. China Ser. B Chem.* **2008**, *51*, 695–699. [\[CrossRef\]](#)
111. Thombre, S.M.; Sarwade, B.D. Synthesis and biodegradability of polyaspartic acid: A critical review. *J. Macromol. Sci. Part A* **2005**, *42*, 1299–1315. [\[CrossRef\]](#)
112. Bennett, G.D. A green polymerization of aspartic acid for the undergraduate organic laboratory. *J. Chem. Educ.* **2005**, *82*, 1380. [\[CrossRef\]](#)
113. Gao, Y.; Fan, L.; Ward, L.P.; Liu, Z. Synthesis of polyaspartic acid derivative and evaluation of its corrosion and scale inhibition performance in seawater utilization. *Desalination* **2015**, *365*, 220–226. [\[CrossRef\]](#)
114. Liu, D.; Dong, W.; Li, F.; Hui, F.; Lédion, J. Comparative performance of polyepoxysuccinic acid and polyaspartic acid on scaling inhibition by static and rapid controlled precipitation methods. *Desalination* **2012**, *304*, 1–10. [\[CrossRef\]](#)
115. Euvrard, M.; Martinod, A.; Neville, A. Effects of carboxylic polyelectrolytes on the growth of calcium carbonate. *J. Cryst. Growth* **2011**, *317*, 70–78. [\[CrossRef\]](#)
116. Gabriel, J.D.S.; Tiera, M.J.; Tiera, V.A.D.O. Synthesis, characterization and antifungal activities of amphiphilic derivatives of Diethylaminoethyl Chitosan against *Aspergillus flavus*. *J. Agric. Food Chem.* **2015**, *63*, 5725–5731. [\[CrossRef\]](#)
117. Feng, Y.; Lin, X.; Li, H.; Akkihebbal, K.S.; Sridhar, T.; Suresh, A.K.; Bellare, J.; Wang, H. Synthesis and characterization of chitosan-grafted BPPO ultrafiltration composite membranes with enhanced antifouling and antibacterial properties. *Ind. Eng. Chem. Res.* **2014**, *53*, 14974–14981. [\[CrossRef\]](#)
118. Chung, Y.-C.; Yeh, J.-Y.; Tsai, C.-F. Antibacterial characteristics and activity of water-soluble Chitosan derivatives prepared by the Maillard Reaction. *Molecules* **2011**, *16*, 8504–8514. [\[CrossRef\]](#)
119. Aziz, M.A.; Cabral, J.D.; Brooks, H.J.L.; Moratti, S.C.; Hanton, L.R. Antimicrobial properties of a Chitosan dextran-based hydrogel for surgical use. *Antimicrob. Agents Chemother.* **2011**, *56*, 280–287. [\[CrossRef\]](#)
120. Cheng, S.; Chen, S.; Liu, T.; Chang, X.; Yin, Y. Carboxymethyl chitosan-Cu mixture as an inhibitor used for mild steel in 1.0 M HCl. *Electrochim. Acta* **2007**, *52*, 5932–5938. [\[CrossRef\]](#)
121. Sakai, T.; Sakamoto, T.; Hallaert, J.; Vandamme, E.J. Pectin, pectinase, and protopectinase: Production, properties and applications. *Adv. Appl. Microbiol.* **1993**, *39*, 213–294. [\[CrossRef\]](#)
122. Schweiger, R.G. Acetyl pectates and their reactivity with polyvalent metal ions1. *J. Org. Chem.* **1964**, *29*, 2973–2975. [\[CrossRef\]](#)
123. Hromádková, Z.; Malovikova, A.; Mozes, S.; Sroková, I.E.; Ibringerova, A. Hydrophobically modified pectates as novel functional polymers in food and non-food applications. *BioResources* **2008**, *3*, 71–78.
124. Zaaferany, I. Inhibition of acidic corrosion of iron by some Carrageenan compounds. *Curr. World Environ.* **2006**, *1*, 101–108. [\[CrossRef\]](#)
125. Abd-El-Khalek, D.E.; Abd-El-Nabey, B.A.; Abdel-Kawi, M.A.; Ebrahim, S.; Ramadan, S.R. The inhibition of crystal growth of gypsum and barite scales in industrial water systems using green antiscalant. *Water Supply* **2019**, *19*, 2140–2146. [\[CrossRef\]](#)
126. Castillo, L.; Torin, E.; García, J.A.; Carrasquero, M.; Navas, M.; Vilorio, A. New product for inhibition of calcium carbonate scale in natural gas and oil facilities based on aloe vera: Application in Venezuelan oilfields. In Proceedings of the Latin American and Caribbean Petroleum Engineering Conference (SPE 123007), Cartagena, Columbia, 31 May–3 June 2009. [\[CrossRef\]](#)
127. Belarbi, Z.; Gamby, J.; Makhouloufi, L.; Sotta, B.; Tribollet, B. Inhibition of calcium carbonate precipitation by aqueous extract of *Paronychia argentea*. *J. Cryst. Growth* **2014**, *386*, 208–214. [\[CrossRef\]](#)
128. Miksic, B.A.; Kharshan, M.A.; Furman, A.Y. Vapor corrosion and scale inhibitors formulated from biodegradable and renewable raw materials. In Proceedings of the European Symposium on Corrosion Inhibitors, Ferrara, Italy, 29 August–2 September 2005.
129. Chaussemier, M.; Pourmohtasham, E.; Gelus, D.; Pécou, N.; Perrot, H.; Lédion, J.; Cheap-Charpentier, H.; Horner, O. State of art of natural inhibitors of calcium carbonate scaling. A review article. *Desalination* **2015**, *356*, 47–55. [\[CrossRef\]](#)

130. Bonoli, M.; Bendini, A.; Cerretani, L.; Lercker, G.; Toschi, T.G. Qualitative and semiquantitative analysis of phenolic compounds in extra virgin olive oils as a function of the ripening degree of olive fruits by different analytical techniques. *J. Agric. Food Chem.* **2004**, *52*, 7026–7032. [[CrossRef](#)] [[PubMed](#)]
131. Maciejewska, G.; Zierkiewicz, W.; Adach, A.; Kopacz, M.; Zapala, I.; Bulik, I.; Cies'lak-Golonka, M.; Grabowski, T.; Wietrzyk, J. A typical calcium coordination number: Physico-chemical study, cytotoxicity, DFT calculations and silicopharmacokinetic characteristics of calcium caffeates. *J. Inorg. Biochem.* **2009**, *103*, 1189–1195. [[CrossRef](#)]
132. Lee, O.-H.; Lee, B.-Y.; Lee, J.; Lee, H.-B.; Son, J.-Y.; Park, C.-S.; Shetty, K.; Kim, Y.-C. Assessment of phenolics-enriched extract and fractions of olive leaves and their antioxidant activities. *Bioresour. Technol.* **2009**, *100*, 6107–6113. [[CrossRef](#)]
133. Mehdi pour, M.; Ramezanzadeh, B.; Arman, S.Y. Electrochemical noise investigation of aloe plant extract as green inhibitor on the corrosion of stainless steel in 1 M H₂SO₄. *J. Ind. Eng. Chem.* **2015**, *21*, 318–327. [[CrossRef](#)]
134. Hassan, K.H.; Khadom, A.A.; Kurshed, N.H. Citrus aurantium leaves extracts as a sustainable corrosion inhibitor of mild steel in sulfuric acid. *S. Afr. J. Chem. Eng.* **2016**, *22*, 1–5. [[CrossRef](#)]
135. Li, L.; Zhang, X.; Lei, J.; He, J.; Zhang, S.; Pan, F. Adsorption and corrosion inhibition of Osmanthus fragrance leaves extract on carbon steel. *Corros. Sci.* **2012**, *63*, 82–90. [[CrossRef](#)]
136. Vioria, A.; Castillo, L.; Garcia, J.A.; Carrasquero Ordaz, M.A.; Torin, E.V. Process Using Aloe for Inhibiting Scale. U.S. Patent 8,039,421 B2, 18 October 2011.
137. Lash, J.E.; Burns, G. Heats of crystallization of CaSO₄·2H₂O. *Bull. Soc. Chim. Belg.* **1984**, *93*, 271–279.
138. Christoffersen, M.; Christoffersen, J.; Weijnen, M.; Van Rosmalen, G. Crystal growth of calcium sulphate dihydrate at low supersaturation. *J. Cryst. Growth* **1982**, *58*, 585–595. [[CrossRef](#)]
139. Chesters, S.P. Innovations in the inhibition and cleaning of reverse osmosis membrane scaling and fouling. *Desalination* **2009**, *238*, 22–29. [[CrossRef](#)]
140. Greenberg, G.; Hasson, D.; Semiat, R. Limits of RO recovery imposed by calcium phosphate precipitation. *Desalination* **2005**, *183*, 273–288. [[CrossRef](#)]
141. Zach-Maor, A.; Semiat, R.; Rahardianto, A.; Cohen, Y.; Wilson, S.; Gray, S. Diagnostic analysis of RO desalting treated wastewater. *Desalination* **2008**, *230*, 239–247. [[CrossRef](#)]
142. Kubo, S.; Takahashi, T.; Morinaga, H.; Ueki, H. Inhibition of calcium phosphate scale on heat exchanger: The relation between laboratory test results and tests on heat transfer surfaces. *Corrosion* **1979**, *79*, 15.
143. Qin, J.J.; Wai, M.N.; Oo, M.H.; Kekre, K.A.; Seah, H. Impact of anti-scalant on fouling of reverse osmosis membranes in reclamation of secondary effluent. *Water Sci. Technol.* **2009**, *60*, 2767–2774. [[CrossRef](#)]
144. Znini, M.; Majidi, L.; Bouyanzer, A.; Paolini, J.; Desjobert, J.-M.; Costa, J.; Hammouti, B. Essential oil of salvia aucheri mesatlantica as a green inhibitor for the corrosion of steel in 0.5M H₂SO₄. *Arab. J. Chem.* **2012**, *5*, 467–474. [[CrossRef](#)]
145. Al-Shammiri, M.; Safar, M.; Al-Dawas, M. Evaluation of two different antiscalants in real operation at the Doha research plant. *Desalination* **2000**, *128*, 1–16. [[CrossRef](#)]
146. Turek, M.; Mitko, K.; Piotrowski, K.; Dydo, P.; Laskowska, E.; Jakóbi-Kolon, A. Agata prospects for high water recovery membrane desalination. *Desalination* **2017**, *401*, 180–189. [[CrossRef](#)]
147. Shemer, H.; Hasson, D. Characterization of the inhibitory effectiveness of environmentally friendly anti-scalants. *Desalin. Water Treat.* **2014**, *55*, 3478–3484. [[CrossRef](#)]
148. Hasson, D.; Shemer, H.; Sher, A. State of the art of friendly “green” scale control inhibitors: A review article. *Ind. Eng. Chem. Res.* **2011**, *50*, 7601–7607. [[CrossRef](#)]
149. Lattemann, S.; Höpner, T. Environmental impact and impact assessment of seawater desalination. *Desalination* **2008**, *220*, 1–15. [[CrossRef](#)]
150. Kroiss, H.; Rechberger, H.; Egle, L. Phosphorus in water quality and waste management. *Integr. Waste Manag.* **2011**, *II*. [[CrossRef](#)]
151. Liu, Y.; Zhou, Y.; Yao, Q.; Huang, J.; Liu, G.; Wang, H.; Cao, K.; Chen, Y.; Bu, Y.; Wu, W.; et al. Double-hydrophilic polyether antiscalant used as a crystal growth modifier of calcium scales in cooling-water systems. *J. Appl. Polym. Sci.* **2013**, *131*, 39792. [[CrossRef](#)]
152. Fu, C.; Zhou, Y.; Liu, G.; Huang, J.; Sun, W.; Wu, W. Inhibition of Ca₃(PO₄)₂, CaCO₃, and CaSO₄ precipitation for industrial recycling water. *Ind. Eng. Chem. Res.* **2011**, *50*, 10393–10399.

153. Ling, L.; Zhou, Y.; Huang, J.; Yao, Q.; Liu, G.; Zhang, P.; Sun, W.; Wu, W. Carboxylate-terminated double-hydrophilic block copolymer as an effective and environmental inhibitor in cooling water systems. *Desalination* **2012**, *304*, 33–40. [\[CrossRef\]](#)
154. Zhang, H.; Cai, Z.; Jin, X.; Sun, D.; Wang, D.; Yang, T.; Zhang, J.; Han, X. Preparation of modified oligochitosan and evaluation of its scale inhibition and fluorescence properties. *J. Appl. Polym. Sci.* **2015**, *132*, 42518. [\[CrossRef\]](#)
155. Zeng, D.; Chen, T.; Zhou, S. Synthesis of polyaspartic acid/chitosan graft copolymer and evaluation of its scale inhibition and corrosion inhibition performance. *Int. J. Electrochem. Sci.* **2015**, *10*, 9513–9527.
156. Cao, K.; Huang, J.; Zhou, Y.; Liu, G.; Wang, H.; Yao, Q.; Liu, Y.; Sun, W.; Wu, W. A multicarboxyl antiscalant for calcium phosphate and calcium carbonate deposits in cooling water systems. *Desalin. Water Treat.* **2013**, *52*, 7258–7264. [\[CrossRef\]](#)
157. Abd-El-Khalek, D.; Abd-El-Nabey, B.; Abdel-Kawi, M.A.; Ramadan, S. Investigation of a novel environmentally friendly inhibitor for calcium carbonate scaling in cooling water. *Desalin. Water Treat.* **2014**, *57*, 1–7. [\[CrossRef\]](#)
158. Maher, Y.A.; Ali, M.E.; Salama, H.E.; Sabaa, M.W. Preparation, characterization and evaluation of chitosan biguanidine hydrochloride as a novel antiscalant during membrane desalination process. *Arab. J. Chem.* **2020**, *13*, 2964–2981. [\[CrossRef\]](#)
159. Harris, A.; Marshall, A. The evaluation of scale control additives. In Proceedings of the Conference on Progress in the Prevention of Fouling in Industrial Plant, University of Nottingham, Nottingham, UK, 1–3 April 1981.
160. Manoli, F.; Dalas, E. The effect of sodium alginate on the crystal growth of calcium carbonate. *J. Mater. Sci. Mater. Electron.* **2002**, *13*, 155–158. [\[CrossRef\]](#) [\[PubMed\]](#)
161. Zhao, Y.; Jia, L.; Liu, K.; Gao, P.; Ge, H.; Fu, L. Inhibition of calcium sulfate scale by poly (citric acid). *Desalination* **2016**, *392*, 1–7. [\[CrossRef\]](#)
162. Xue, X.; Fu, C.; Li, N.; Zheng, F.; Yang, W.; Yang, X. Performance of a non-phosphorus antiscalant on inhibition of calcium-sulfate precipitation. *Water Sci. Technol.* **2012**, *66*, 193–200. [\[CrossRef\]](#) [\[PubMed\]](#)
163. Zhao, Y.; Liang, Y.; Liu, Y.; Zhang, X.; Hu, X.; Tu, S.; Wu, A.; Zhang, C.; Zhong, J.; Zhao, S.; et al. Isolation of broad-specificity domain antibody from phage library for development of pyrethroid immunoassay. *Anal. Biochem.* **2016**, *502*, 1–7. [\[CrossRef\]](#) [\[PubMed\]](#)
164. Li, H.-Y.; Ma, W.; Wang, L.; Liu, R.; Wei, L.-S.; Wang, Q. Inhibition of calcium and magnesium-containing scale by a new antiscalant polymer in laboratory tests and a field trial. *Desalination* **2006**, *196*, 237–247. [\[CrossRef\]](#)
165. El-Etre, A. Khillah extract as inhibitor for acid corrosion of SX 316 steel. *Appl. Surf. Sci.* **2006**, *252*, 8521–8525. [\[CrossRef\]](#)
166. Raja, P.B.; Fadaeinasab, M.; Qureshi, A.K.; Rahim, A.A.; Osman, H.; Litaudon, M.; Awang, K. Evaluation of green corrosion inhibition by alkaloid extracts of ochrosia oppositifolia and isoreserpiline against Mild Steel in 1 M HCl Medium. *Ind. Eng. Chem. Res.* **2013**, *52*, 10582–10593. [\[CrossRef\]](#)
167. Mpelwa, M.; Tang, S.-F. State of the art of synthetic threshold scale inhibitors for mineral scaling in the petroleum industry: A review. *Pet. Sci.* **2019**, *16*, 830–849. [\[CrossRef\]](#)

